Final Results from the QWeak Experiment

David S. Armstrong
William & Mary

for the QWeak Collaboration

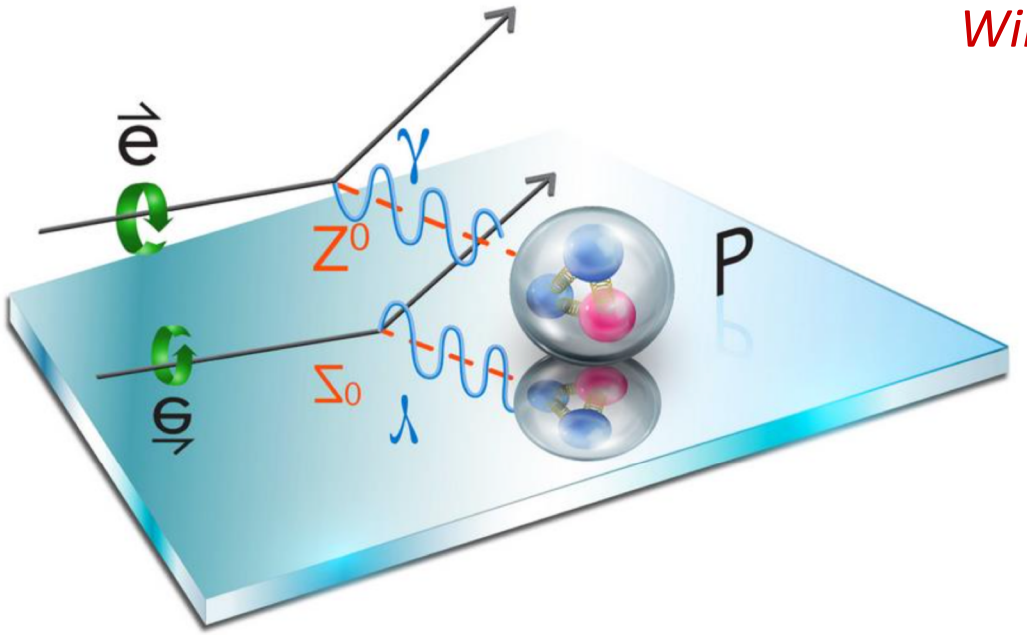

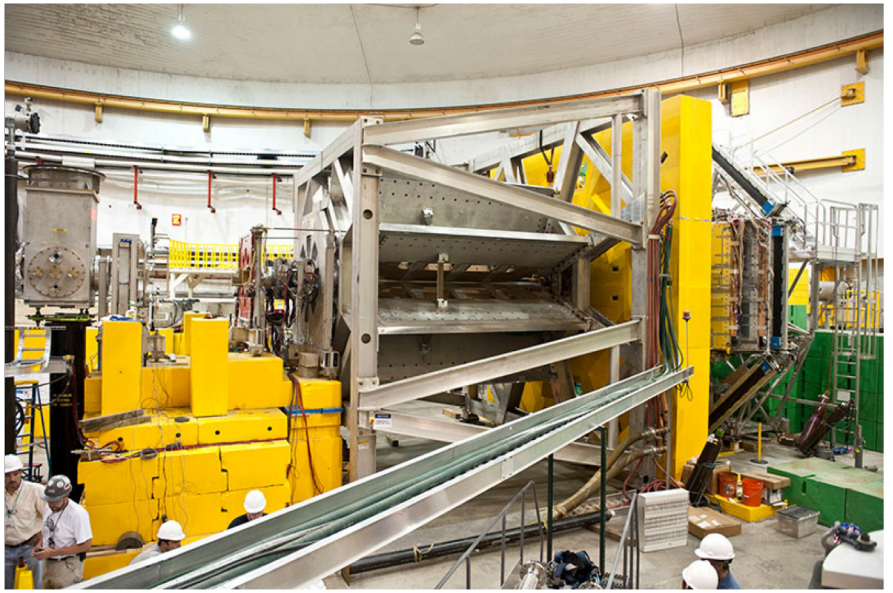

PVES 2018 Workshop
MITP/Univ. Mainz April 24 2018

Search for physics *Beyond the Standard Model*

- Received Wisdom: Standard Model is incomplete, and is low-energy effective theory of more fundamental physics
- Low energy ($Q^2 << M^2$): Precision Frontier complementary to Energy Frontier measurements (LHC)

- ***Neutrino masses and role in the early universe*** 0νββ *decay,* θ_{13}, β *decay,…*
- ***Matter-antimatter asymmetry in the present universe*** *EDM, DM, LFV,* 0νββ, θ_{13}
- ***Unseen Forces of the early Universe*** *Weak decays,* ***PVES****,* g_μ*-2,…*

Any LHC new physics signals likely need additional indirect measurements to pin down their nature

- ***Neutrons:*** *Lifetime, P- & T-Violating Asymmetries* *[LANSCE, Grenoble, NIST, SNS...]*
- ***Muons:*** *Lifetime, Michel parameters, g-2, Mu2e* *[PSI, TRIUMF, FNAL, J-PARC...]*
- ***PVES:*** *Low-energy weak neutral current couplings, precision weak mixing angle* *[SLAC, Jefferson Lab, Mainz]*
- ***Atoms:*** *atomic parity violation*

Idea - *select observables that are:*

1) zero, or significantly suppressed, in Standard Model

2) Robust predictions within Standard Model

PVES: Brief History

Pioneering (1978) early SM tests
SLAC E122 PVDIS – Prescott *et al.*
A = -152 ppm
Bates 12C, Mainz Be

Strange Form Factors (1998 –2009)
SAMPLE, HAPPEX, G0, A4
A ~ 1 – 50 ppm

Standard Model Tests (2003 - present)
SLAC E158 Moller: A = - 131 ppb JLAB
Qweak: A ~ -230 ppb
→ smaller asymmetries,
smaller absolute & relative errors

Future: Standard Model, Neutron radius, hadron structure studies:
MOLLER, P2@MESA, SOLID,
12C@MESA, PREX-II, CREX

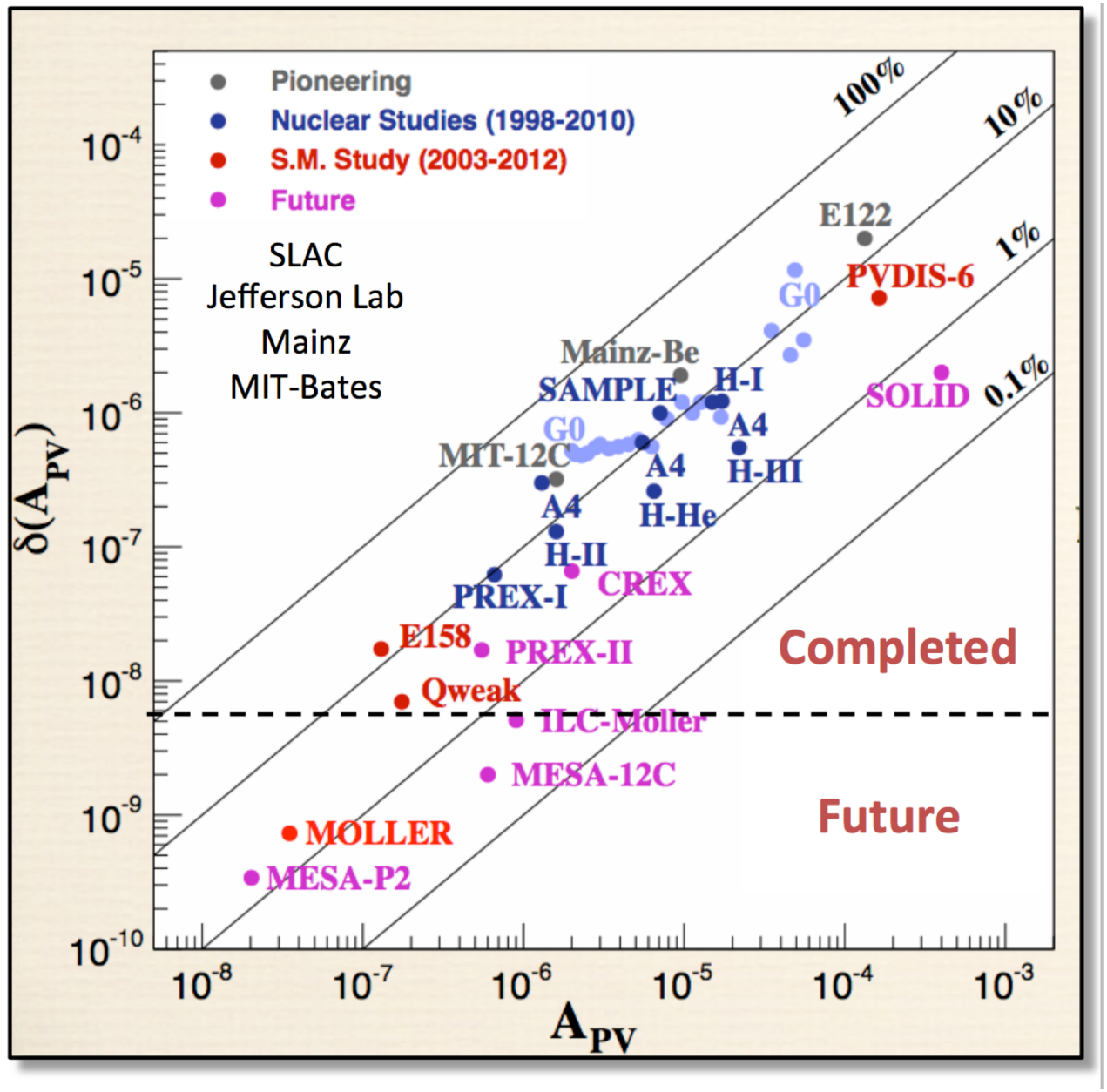

Figure courtesy of Kent Paschke

Weak Charge

Electroweak Lagrangian → Parity-Violating neutral-current electron-quark term:

$$\mathcal{L}_{PV}^{EW} = \frac{G_F}{\sqrt{2}}\left[g_A^e(\bar{e}\gamma_\mu\gamma_5 e)\cdot\sum_q g_V^q(\bar{q}\gamma^\mu q) + g_V^e(\bar{e}\gamma_\mu e)\cdot\sum_q g_A^q(\bar{q}\gamma^\mu\gamma_5 q)\right]$$

$$C_{1q} = 2g_A^e g_V^q$$

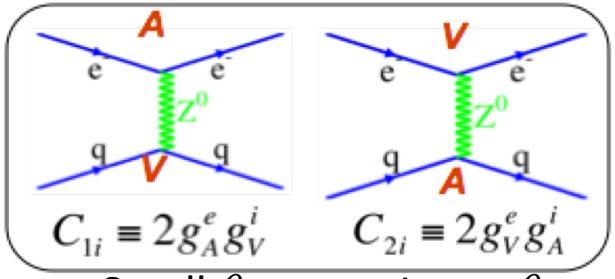

Small θ Large θ

-Electroweak Charges-

Particle	Electric Charge	Weak Vector Charge ($\sin^2\theta_W \approx \frac{1}{4}$)
u	$+\frac{2}{3}$	$-2C_{1u} = +1 - \frac{8}{3}\sin^2\theta_W \approx +\frac{1}{3}$
d	$-\frac{1}{3}$	$-2C_{1d} = -1 + \frac{4}{3}\sin^2\theta_W \approx -\frac{2}{3}$
p(uud)	$+1$	$Q_W^p = 1 - 4\sin^2\theta_W \approx 0$ ← Proton's Weak Charge
n(udd)	0	$Q_W^n = -1$

Weak Charge Triad in Neutral Current Studies

C_{1u} , C_{1d} , C_{ee} : "Weak Charges": neutral current analog to the electric charges

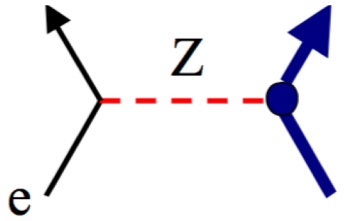

Electron's weak charge: $Q_W^e \equiv -2C_{ee} = -(1-4\sin^2\theta_W)$

parity-violating Møller scattering $\vec{e} + e \rightarrow e + e$

- published: **SLAC E158** ~ 13% on Q^e_W

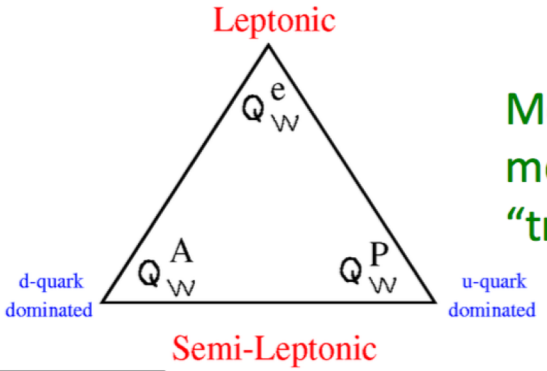

Most precise low energy measurements define a weak charge "triad" (M. Ramsey-Musolf)

"Neutron's weak charge":

$$Q_W^A(Z,N) \equiv -2\left[C_{1u}(2Z+N) + C_{1d}(Z+2N)\right]$$
$$\approx Z\left(1-4\sin^2\theta_W\right) - N \approx -N$$

Atomic parity violation

- published: **^{133}Cs** ~ 0.6% on Q^A_W

Proton's weak charge:

$$Q_W^p \equiv -2\left[2C_{1u} + C_{1d}\right] = \left(1-4\sin^2\theta_W\right)$$

parity-violating elastic ep scattering

$\vec{e} + p \rightarrow e + p$

- **Results today: JLab Qweak ~ 6% on Q^p_W**

Q^e_W and Q^p_W are suppressed in Standard Model → increased sensitivity to new physics.
ie. 6% on Q^p_W=0.0708 sensitive to new neutral current amplitudes as weak as ~ $4\times10^{-3}\ G_F$

PVES: Parity-violating electron scattering

Scatter longitudinally-polarized electrons from unpolarized target
Originally proposed by Ya. B. Zeldovich JETP 36 (1959)

Electroweak interference

$$A \equiv \frac{d\sigma_+ - d\sigma_-}{d\sigma_+ + d\sigma_-} \rightarrow \frac{\left| \gamma \right| \left| \gamma + Z^0 \right|}{\left| \gamma \right|^2}$$

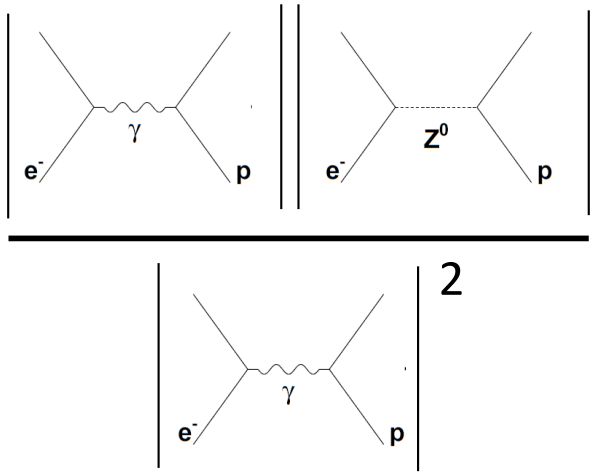

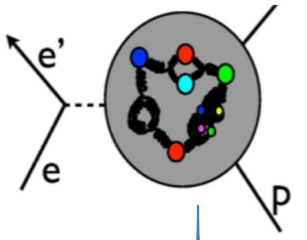

For e-p scattering:

$$A \equiv \frac{d\sigma_+ - d\sigma_-}{d\sigma_+ + d\sigma_-} \xrightarrow[\theta \to 0]{Q^2 \to 0} \left[\frac{-G_F}{4\pi\alpha\sqrt{2}}\right]\left[Q^2\, Q^p_{weak} + Q^4 B\left(Q^2\right)\right]$$

For forward angle scattering at low Q^2 :
A_{PV} accesses Q^p_W

"Form factor" term due to finite proton size – hadronic structure (~ 30% for Qweak) – determined well by existing PVES high-Q^2 data

QWeak: History

QWeak Experiment:
Hall C at Jefferson Lab

(Newport News, VA, USA)

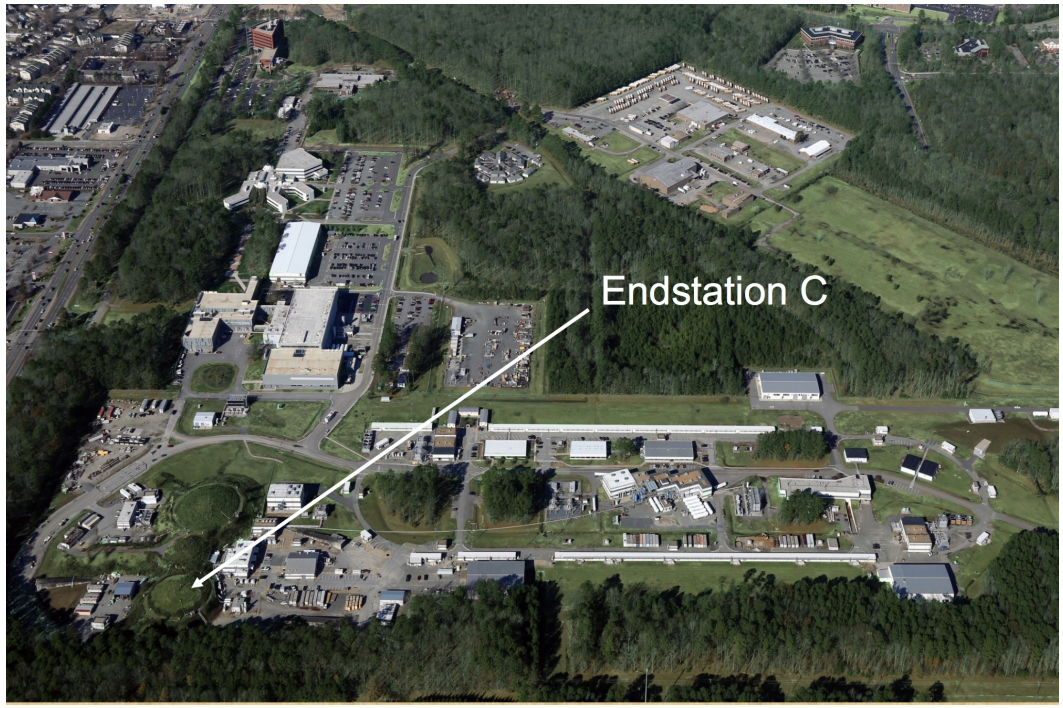

- Initial organizational meeting: 2000
- Proposal: 2001
- Design/construction: 2003 – 2010
- Data-taking: 2010 – 2012
  (~ 1 year total beam time)
- Two main Runs, separated by
  6-month down.

•• Last experiment in Hall C in "6 GeV era" CEBAF
•• First results on proton's weak charge (based on first 4% of the dataset)
published in **Phys. Rev. Lett. 111, 141803 (2013)**
•• Apparatus described in **NIM A781, 105 (2015)**

• Final unblinded results first released at PANIC 2017 (Beijing) by Roger Carlini
September 3, 2017
• Publication in press in *Nature* - *expected ≈ May 10 issue*

Meeting PVES Challenges

$A_{ep} \approx 200\ ppb$ want $\approx 4\%$ precision

- 180 μA beam current (JLab record)
- High power cryogenic target
- Rapid helicity reversal (960 Hz)
- Small scattering angle: toroidal magnet, large acceptance
- GHz detected rates: data-taking in integrating mode
- Radiation hard detectors
- Low noise 18-bit ADCs
- Exquisite control of helicity-correlated beam parameters
- Four different kinds of helicity reversal:
  - Rapid (Laser beam at source: Pockels cell)
  - Slow (insertable λ/2 plate in laser beam)
  - Ultra slow (Wien-reversal, g-2 spin flip)
- Two independent high-precision beam polarimeters
- High resolution Beam Current monitors
- Dedicated Tracking system for kinematics determination

The Q_{Weak} Apparatus

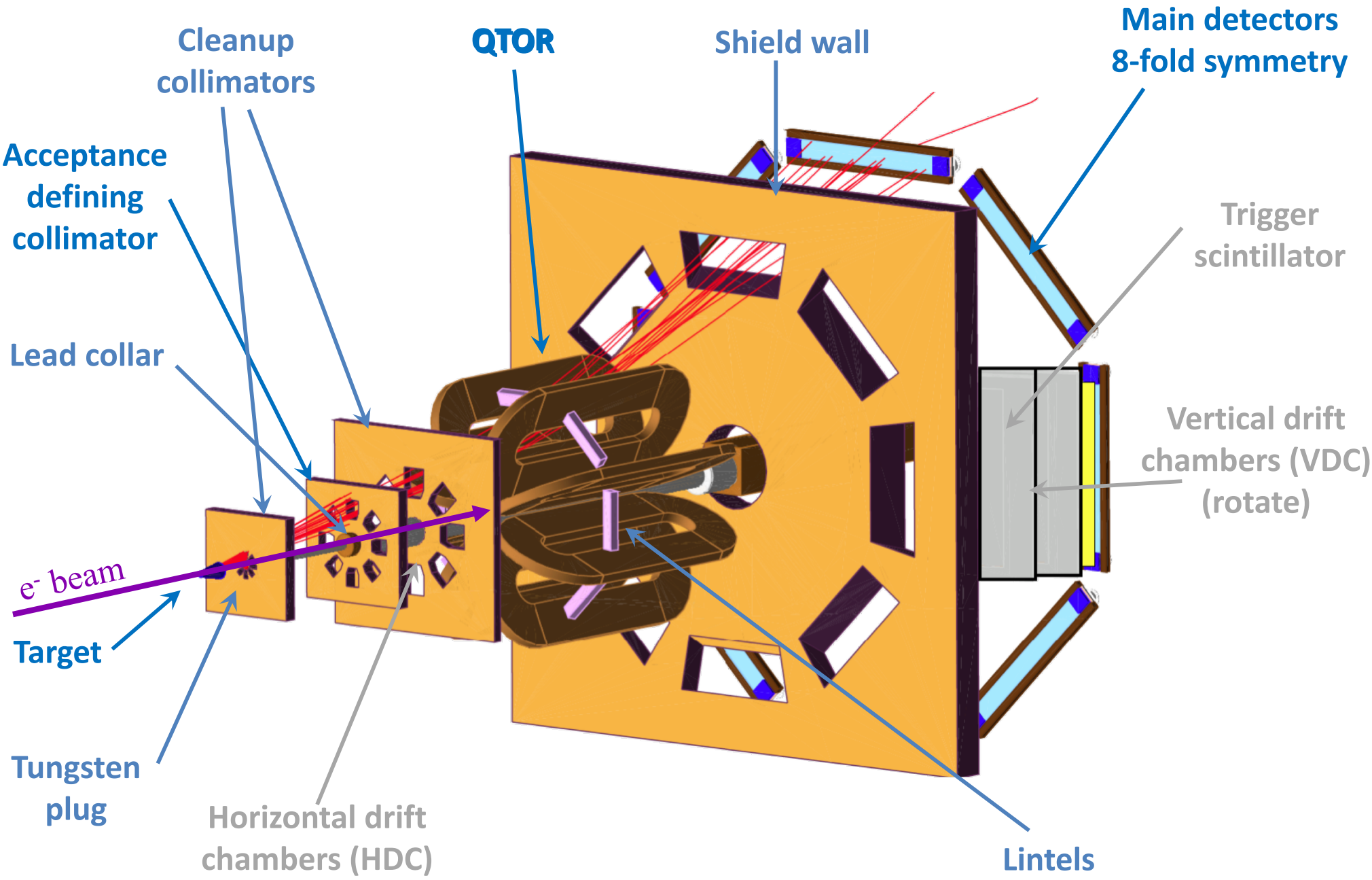

The Q_{Weak} Apparatus – during installation

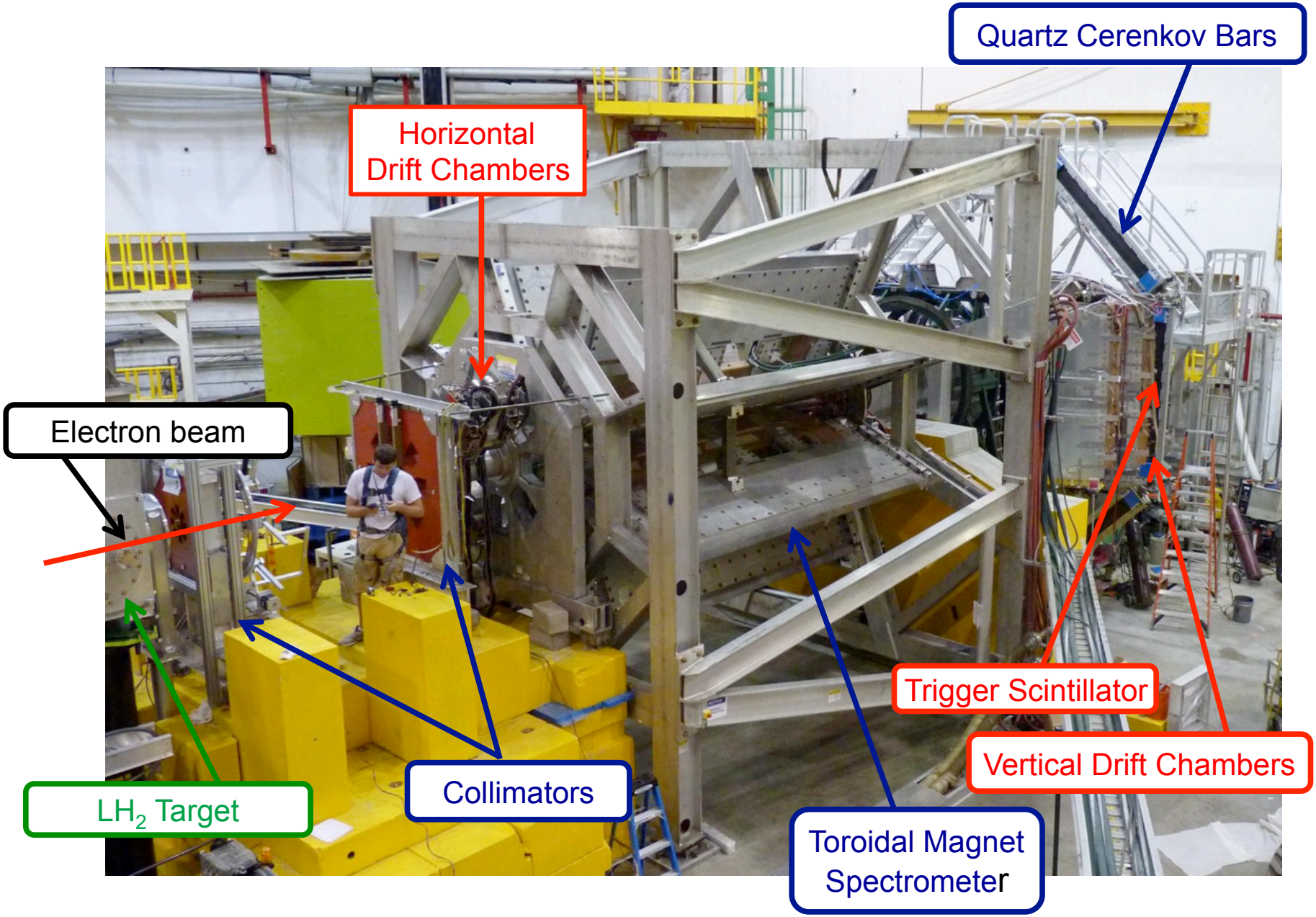

Main Detectors

- Main detectors

  Toroidal magnet focuses elastic electrons onto each bar
  - 8 fused-silica Cerenkov bars: 200 cm x 18 cm x 1.25 cm
  - Rad-hard, low luminescence
  - 900 MHz e^- per detector
  - Azimuthal symmetry maximizes rates & reduces systematic uncertainties
  - 2 cm lead pre-radiators: a) reduce soft backgrounds discovered in commissioning
    b) boost signal size (but cost to energy resolution)

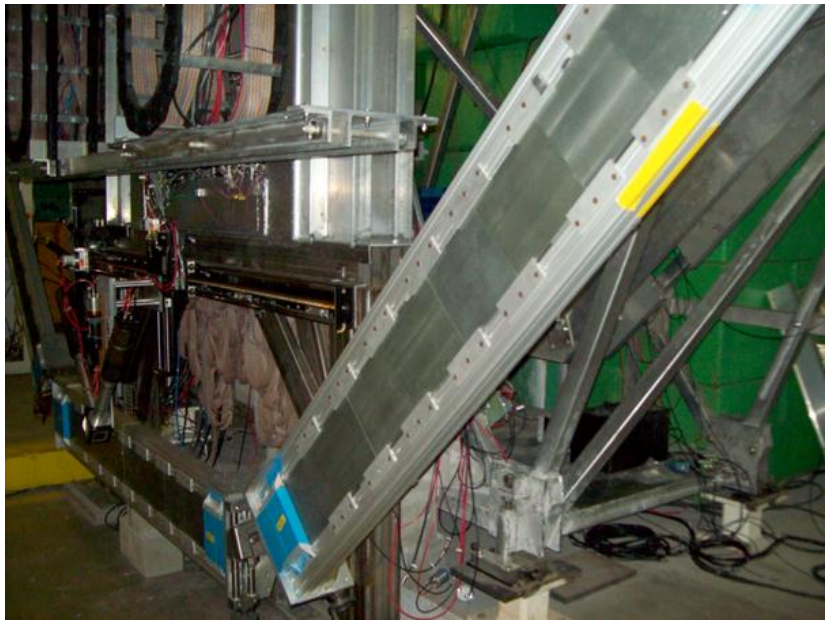

Close up of one detector *in situ*

Simulation of scattering rate MD face

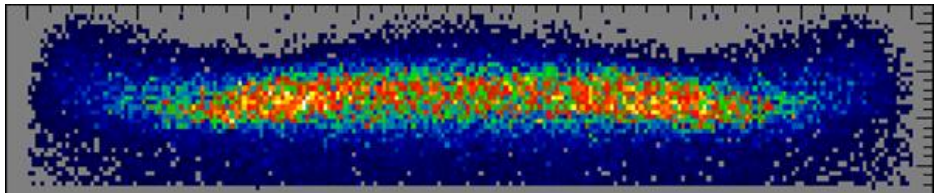

Measured

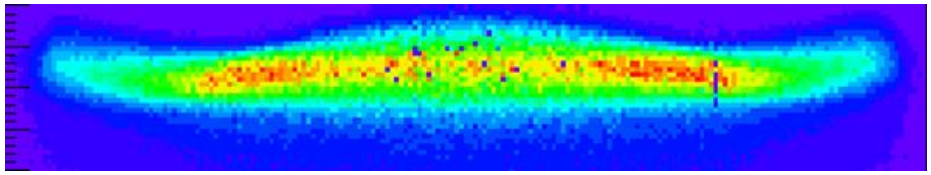

Hydrogen Target

35 cm, 2.5 kW liquid hydrogen target (world's highest power cryotarget)

Designed using Computational Fluid Dynamics

- Temperature ~20 K
- Pressure: 220 kPa
- Beam: 150 – 180 μA
- 4% X_0

Target boiling might have been problematic!

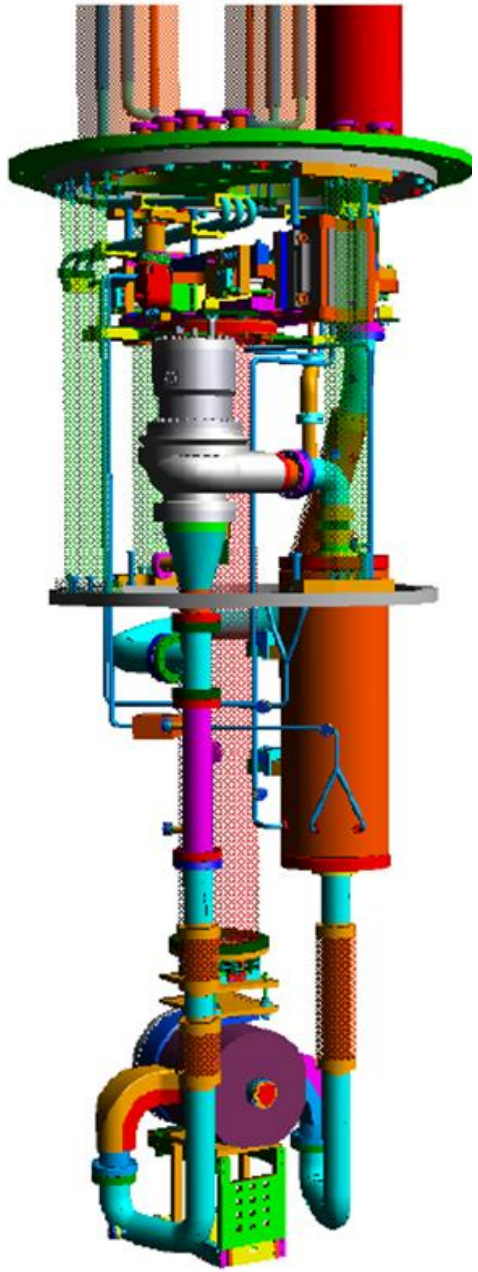

Rapid helicity-reversal: 960 Hz

common-mode rejection of boiling noise

Achieved ~50 ppm noise (< 225 ppm counting statistics)

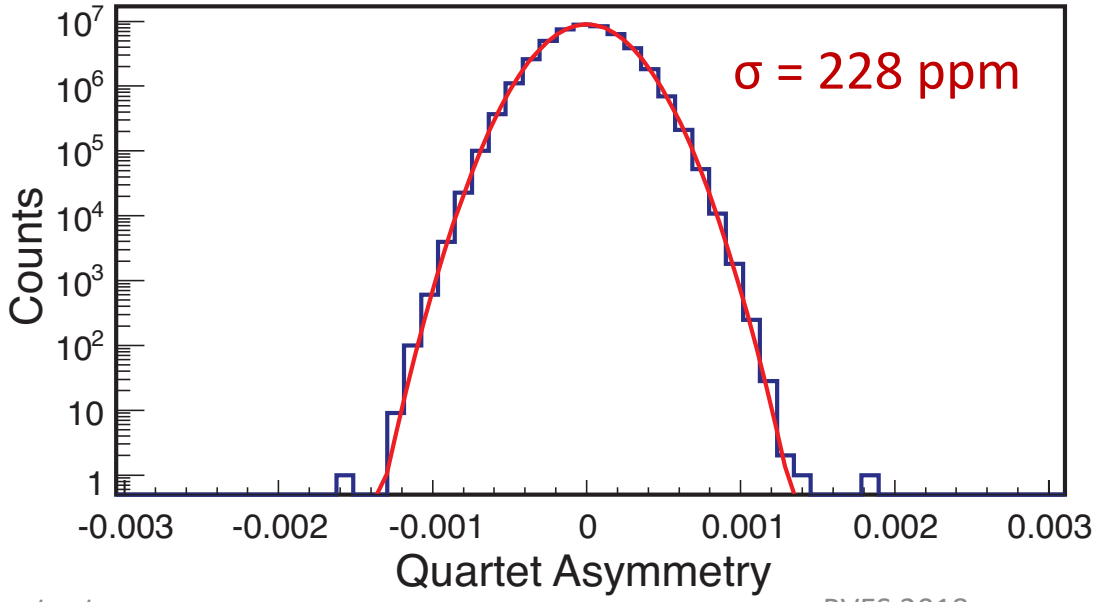

Beam Polarimetry

Møller polarimeter $(\vec{e} + \vec{e} \rightarrow e + e)$

- Precise, but invasive
- Thin, polarized Fe target
- Brute force polarization
- Limited to low current

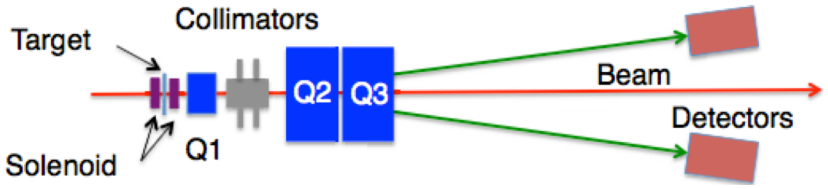

Compton polarimeter $(\vec{e} + \gamma \rightarrow e + \gamma)$

- Installed for Q-weak
- Runs continuously at high currents
- Statistical precision: 1% per hour
- Electron Detector: Diamond strips

Detect *both* recoil electron and photon.

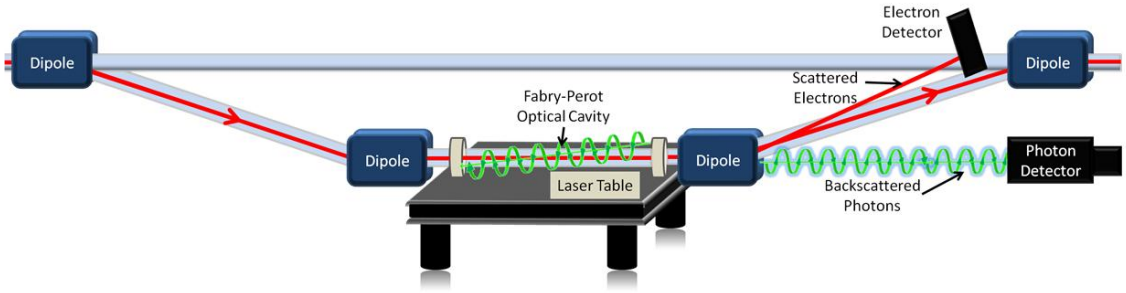

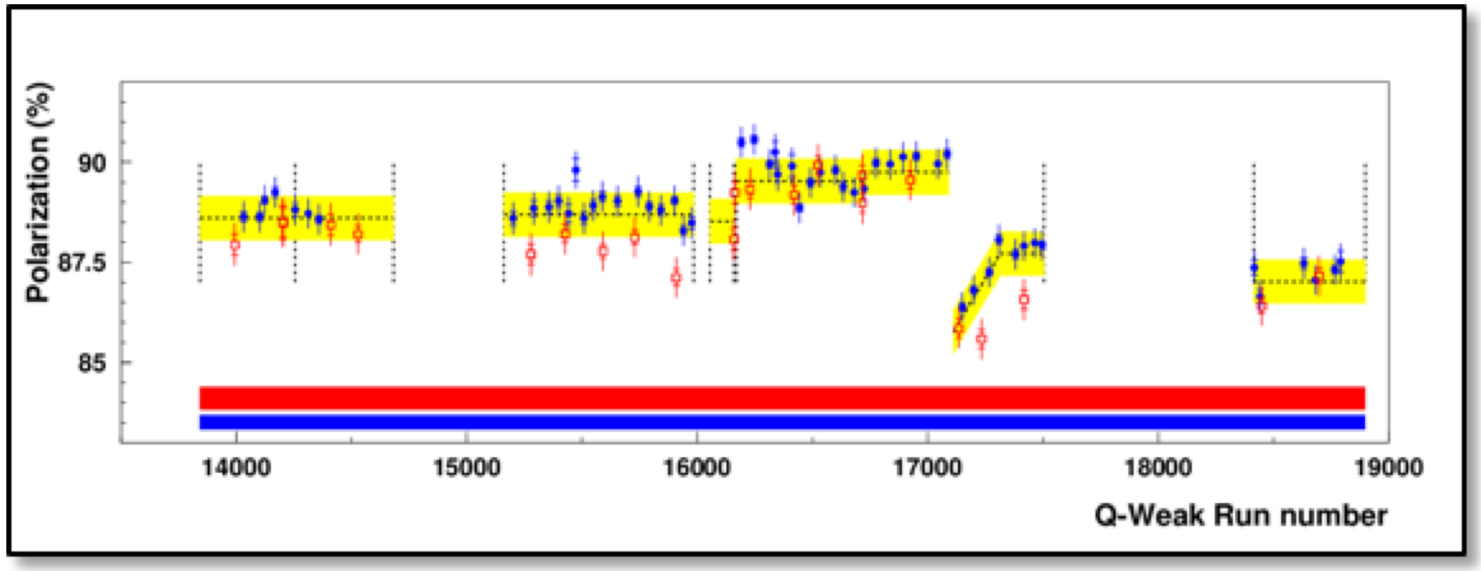

0.6% precision achieved in Run 2

Phys. Rev. X **6**, 011013 (2016)

Phys. Lett. B **766**, 339 (2017)

Helicity-Correlated Beam Parameter Sensitivities

$A_{beam} = \sum_i \frac{\partial A}{\partial \chi_i} \Delta \chi_i$
where i runs over x,y,x'(angle),y'(angle), and energy.

Need to determine the sensitivities: $\frac{\partial A}{\partial \chi_i}$

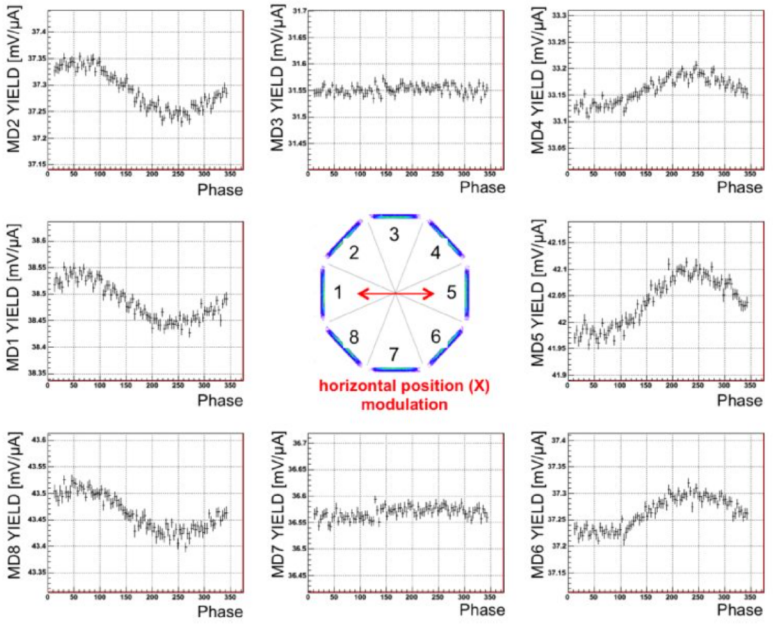

Natural: Linear regression of natural beam motion

Driven: Drive sinusoidal beam oscillations with large amplitude

Beam Parameter	Run 1 $\Delta\chi_i$	Run 2 $\Delta\chi_i$	Typical $\partial A/\partial\chi_i$
X	-3.5 ± 0.1 nm	-2.3 ± 0.1 nm	-2 ppb/nm
X'	-0.30 ± 0.01 nrad	-0.07 ± 0.01 nrad	50 ppb/nrad
Y	-7.5 ± 0.1 nm	0.8 ± 0.1 nm	< 0.2 ppb/nm
Y'	-0.07 ± 0.01 nrad	-0.04 ± 0.01 nrad	< 3 ppb/nrad
Energy	-1.69 ± 0.01 ppb	-0.12 ± 0.01 ppb	-6 ppb/ppb

Run 1: $A_{\text{beam}} = 18.5 \pm 4.1$ ppb Run 2: $A_{\text{beam}} = 0.0 \pm 1.1$ ppb

Target Windows

Background from detected electrons that scattered from thin Aluminum entrance and exit windows:

1. Measure ≈1500 ppb asymmetry from thick dummy target (identical Al alloy).
2. Precisely measure the $(2.52 \pm 0.06)\%$ "dilution" from windows.

- Net correction is ≈20% of hydrogen signal: 1.2% uncertainty on result

Aluminum Parity-Violating Asymmetry

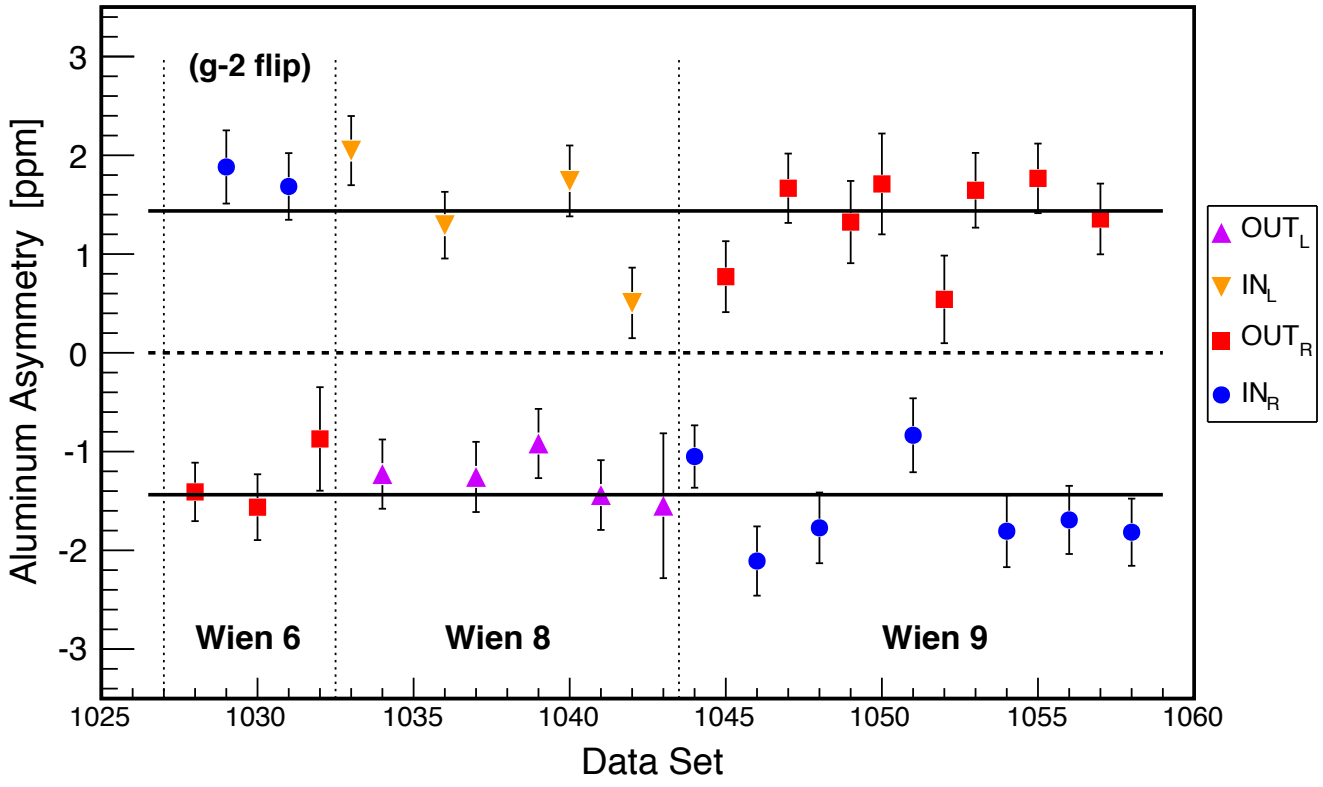

Statistical error: 5.0%
Systematic error: 0.7%

Three slow reversal types:

IN/OUT: reversal of laser helicity (IWHP)

L/R: reversal of electron beam via Wien filter

g-2 flip: reversal of electron via spin precession in accelerator

Kinematics (Q^2) determination

To determine Q^2, we go to "tracking" mode:

- Currents ~ 50 pA
- Use Vertical + Horizontal Drift Chambers
- Reconstruct individual scattering events

$$A_{PV} = -\frac{G_F Q^2}{4\pi\alpha\sqrt{2}}\{Q_w^p + B(\theta, Q^2)Q^2\}$$

$Q^2 = 0.0249\ (\mathrm{GeV}/c)^2$

$q = 0.80\ \mathrm{fm}^{-1}$

Correct for radiative effects in target with Geant 4 simulations, benchmarked with gas-target & solid target studies

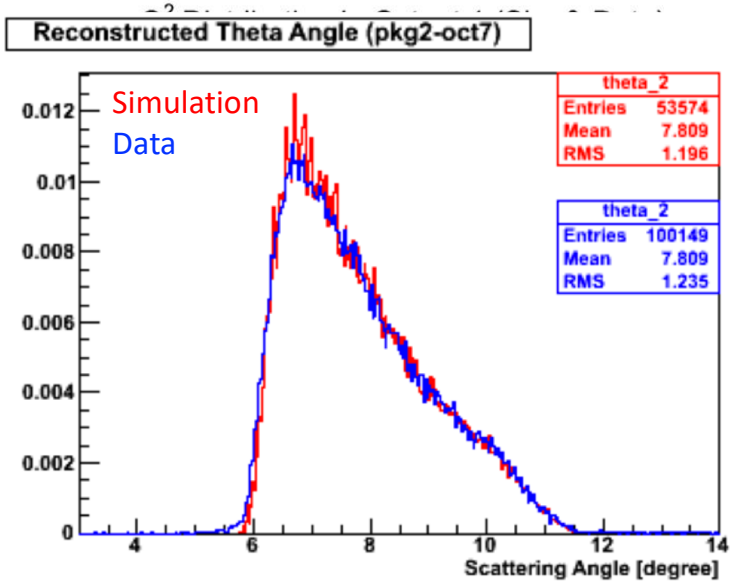

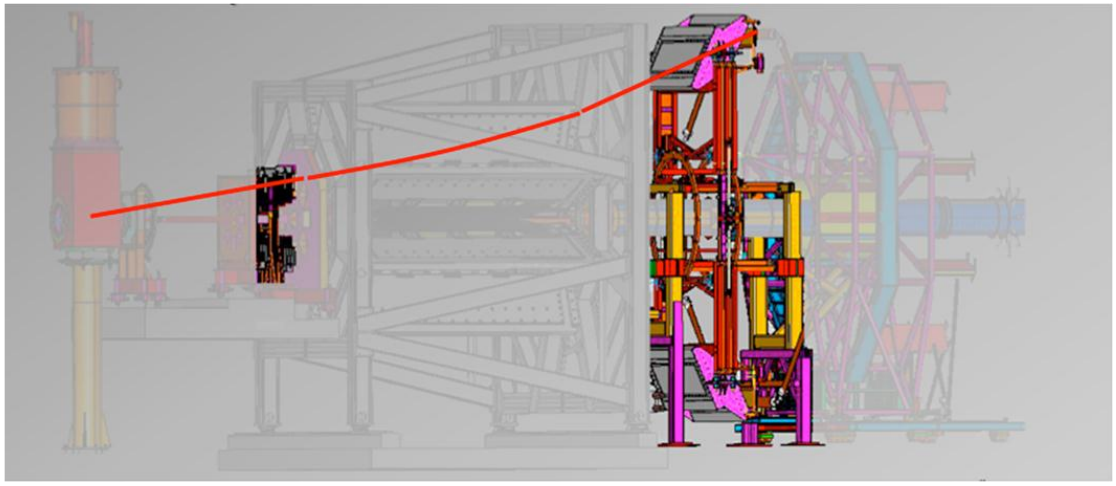

Secondary Scattering

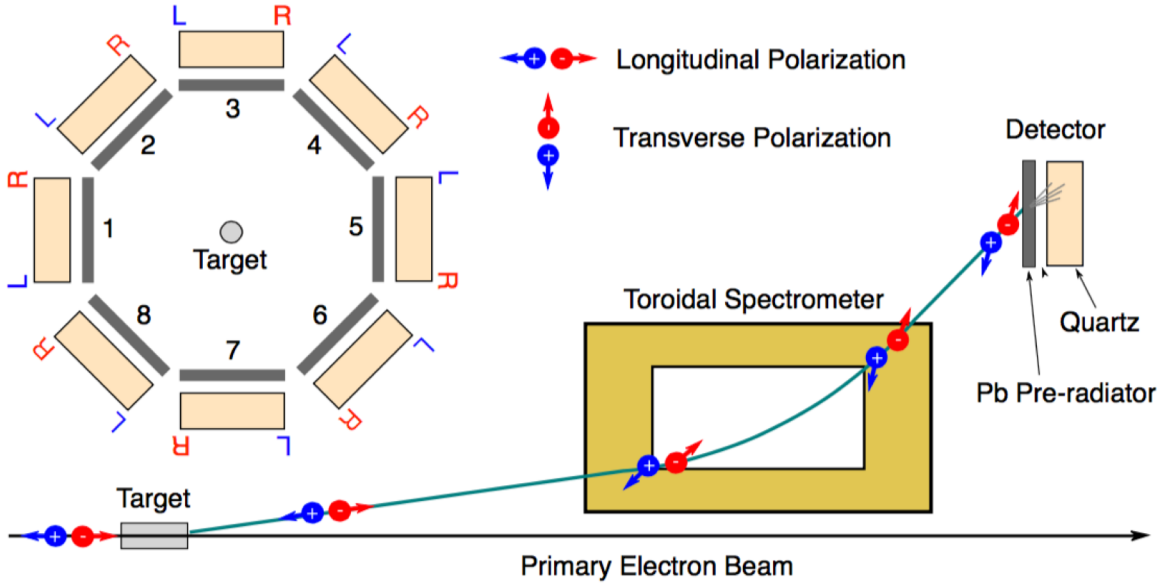

- Spin precession of scattered e^- in magnet: some transverse polarization P_T
- P_T analyzed by scattering in Pb pre-radiators → transverse asymmetry in detectors: opposite sign in the two PMTs (R & L) in each detector

  $A_{diff} = A_R - A_L$ Parity Signal = $\frac{A_R + A_L}{2}$ ∴ Effect cancels to first order

- Analyzing power in Pb:
  1. Beam-normal single spin asymmetry (high energy): 2γ exchange
  2. Mott scattering (low energy in shower) → dominant effect

  A_{diff} is of same scale (hundreds of ppb) as A_{PV}

Secondary Scattering

- This transverse asymmetry couples with position & angle dependence of optical response of detectors.
- Any non-cancellation between R and L PMTs: detector imperfections & non-symmetric flux distributions.
- Optical properties and flux distributions measured with tracking system.
- Quantified small non-cancellation with detailed GEANT 4 simulation.

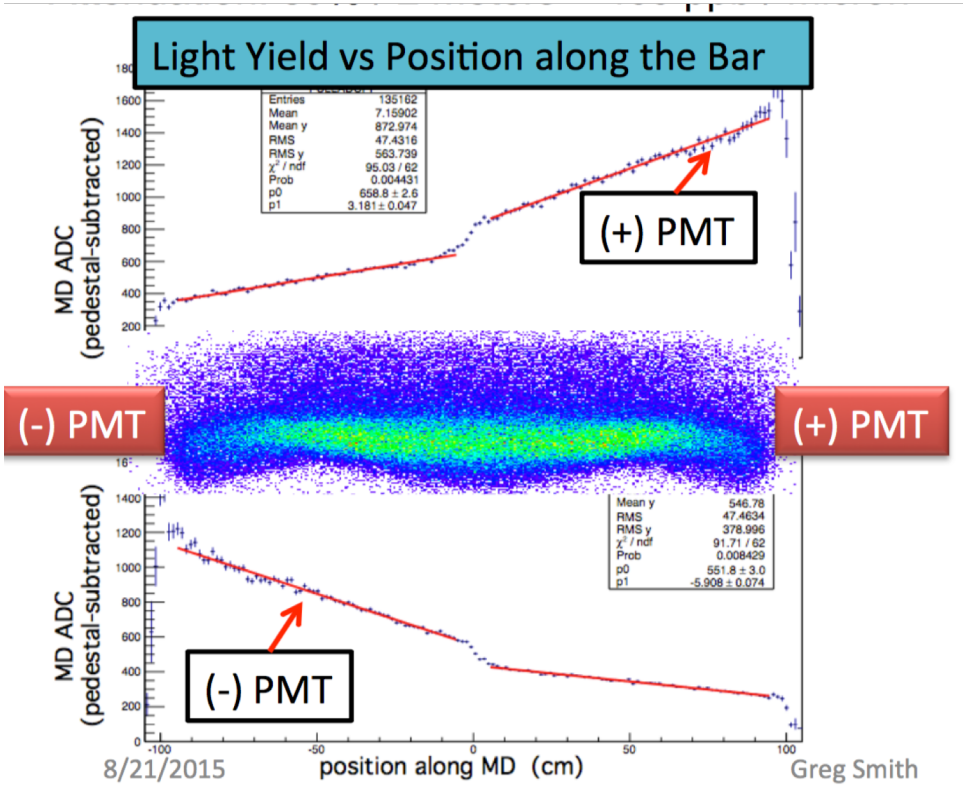

Contributions to A_{bias} Uncertainty

Optical Model:	± 2.7 ppb
Simulation cross checks:	± 2.3 ppb
Glue Joints Effects:	± 1.5 ppb
Effective Model:	±1.5 ppb
A_{bias} Correction	**4.3 ± 3.0 ppb**

Asymmetry: Dominant Systematic Uncertainties

Fractions of total systematic error

Quantity	Run 1 error (ppb)	Run 1 fractional	Run 2 error (ppb)	Run 2 fractional
BCM Normalization: $A_{\rm BCM}$	5.1	25%	2.3	17%
Beamline Background: $A_{\rm BB}$	5.1	25%	1.2	5%
Beam Asymmetries: $A_{\rm beam}$	4.7	22%	1.2	5%
Rescattering bias: $A_{\rm bias}$	3.4	11%	3.4	37%
Beam Polarization: P	2.2	5%	1.2	4%
Target windows: A_{b1}	1.9	4%	1.9	12%
Kinematics: R_{Q^2}	1.2	2%	1.3	5%
Total of others	2.5	6%	2.2	15%
Combined in quadrature	10.1		5.6	

$$A_{\rm msr} = A_{\rm raw} + A_T + A_L + A_{\rm BCM} + A_{\rm BB} + A_{\rm beam} + A_{\rm bias}$$

$$A_{ep} = R_{\rm tot} \frac{A_{\rm msr}/P - \sum_{i=1,3,4} f_i A_i}{1 - \sum_{i=1}^{4} f_i}$$

$$R_{\rm tot} = R_{\rm RC} R_{\rm Det} R_{\rm Acc} R_{Q^2}$$

All Corrections to Asymmetry

$$A_{\rm msr} = A_{\rm raw} + A_T + A_L + A_{\rm BCM} + A_{\rm BB} + A_{\rm beam} + A_{\rm bias}$$

$$A_{ep} = R_{\rm tot} \frac{A_{\rm msr}/P - \sum_{i=1,3,4} f_i A_i}{1 - \sum_{i=1}^{4} f_i}$$

f_1: Al f_2: beamline
f_3: neutrals f_4 : inelastics

$$R_{\rm tot} = R_{\rm RC} R_{\rm Det} R_{\rm Acc} R_{Q^2}$$

Quantity	Run 1	Run 2	Correlation
$A_{\rm raw}$	-192.7 ± 13.2 ppb	-170.7 ± 7.3 ppb	—
$A_{\rm T}$	0 ± 1.1 ppb	0 ± 0.7 ppb	0
$A_{\rm L}$	1.3 ± 1.0 ppb	1.2 ± 0.9 ppb	1
$A_{\rm BCM}$	0 ± 4.4 ppb	0 ± 2.1 ppb	0.67
$A_{\rm BB}$	3.9 ± 4.5 ppb	-2.4 ± 1.1 ppb	0
$A_{\rm beam}$	18.5 ± 4.1 ppb	0.0 ± 1.1 ppb	0
$A_{\rm bias}$	4.3 ± 3.0 ppb	4.3 ± 3.0 ppb	1
$A_{\rm msr}$	-164.6 ± 15.5 ppb	-167.5 ± 8.4 ppb	—
P	87.66 ± 1.05 %	88.71 ± 0.55 %	0.19
f_1	2.471 ± 0.056 %	2.516 ± 0.059 %	1
A_1	1.514 ± 0.077 ppm	1.515 ± 0.077 ppm	1
f_2	0.193 ± 0.064 %	0.193 ± 0.064 %	1
f_3	0.12 ± 0.20 %	0.06 ± 0.12 %	1
A_3	-0.39 ± 0.16 ppm	-0.39 ± 0.16ppm	1
f_4	0.018 ± 0.004 %	0.018 ± 0.004 %	1
A_4	-3.0 ± 1.0 ppm	-3.0 ± 1.0ppm	1
$R_{\rm RC}$	1.010 ± 0.005	1.010 ± 0.005	1
$R_{\rm Det}$	0.9895 ± 0.0021	0.9895 ± 0.0021	1
$R_{\rm Acc}$	0.977 ± 0.002	0.977 ± 0.002	1
R_{Q^2}	0.9928 ± 0.0055	1.0 ± 0.0055	1
$R_{\rm tot}$	0.9693 ± 0.0080	0.9764 ± 0.0080	1
$\sum f_i$	2.80 ± 0.22 %	2.78 ± 0.15 %	1

Asymmetry: Dominant Corrections

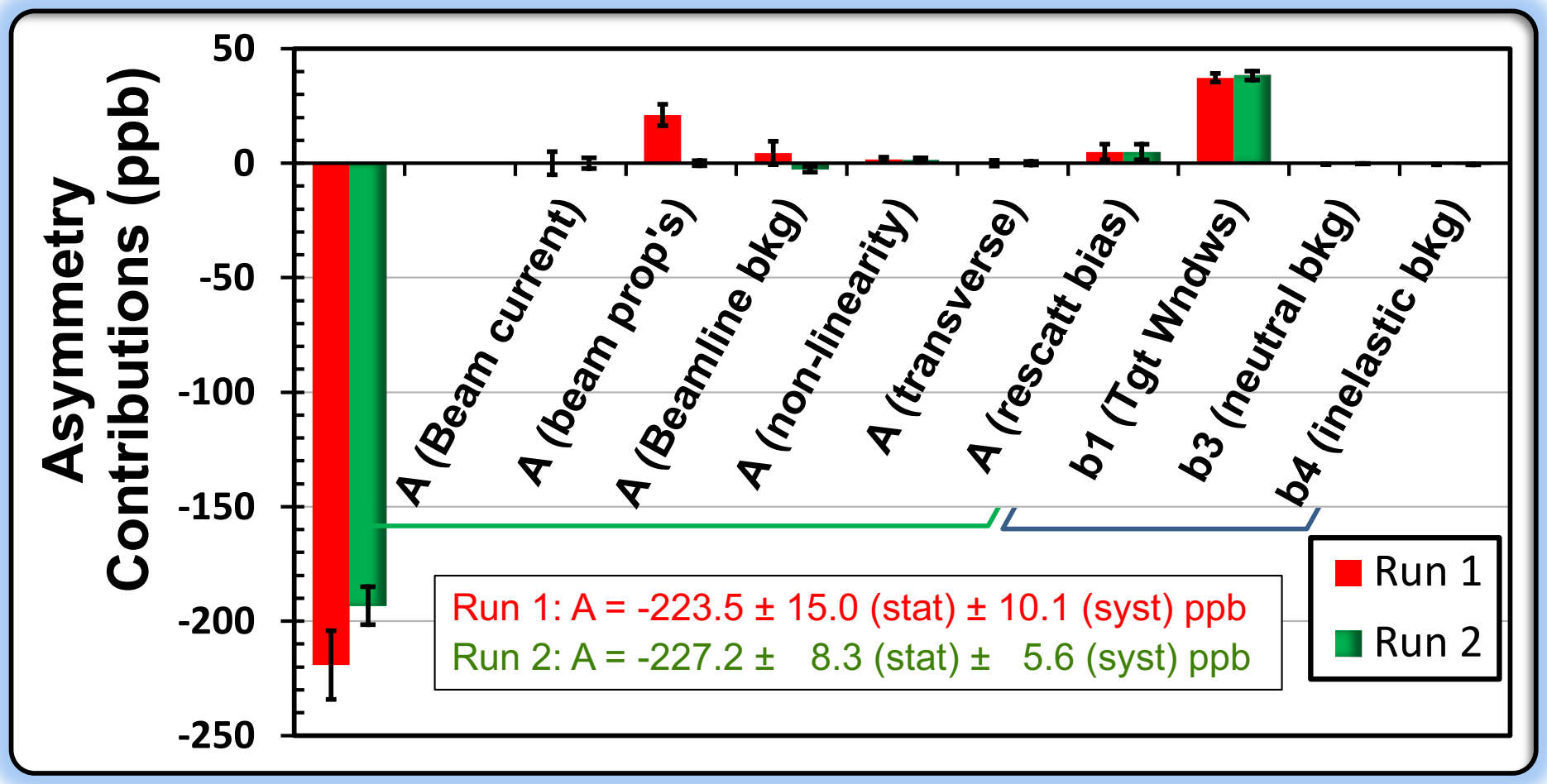

Behavior of Asymmetry under Slow Reversals

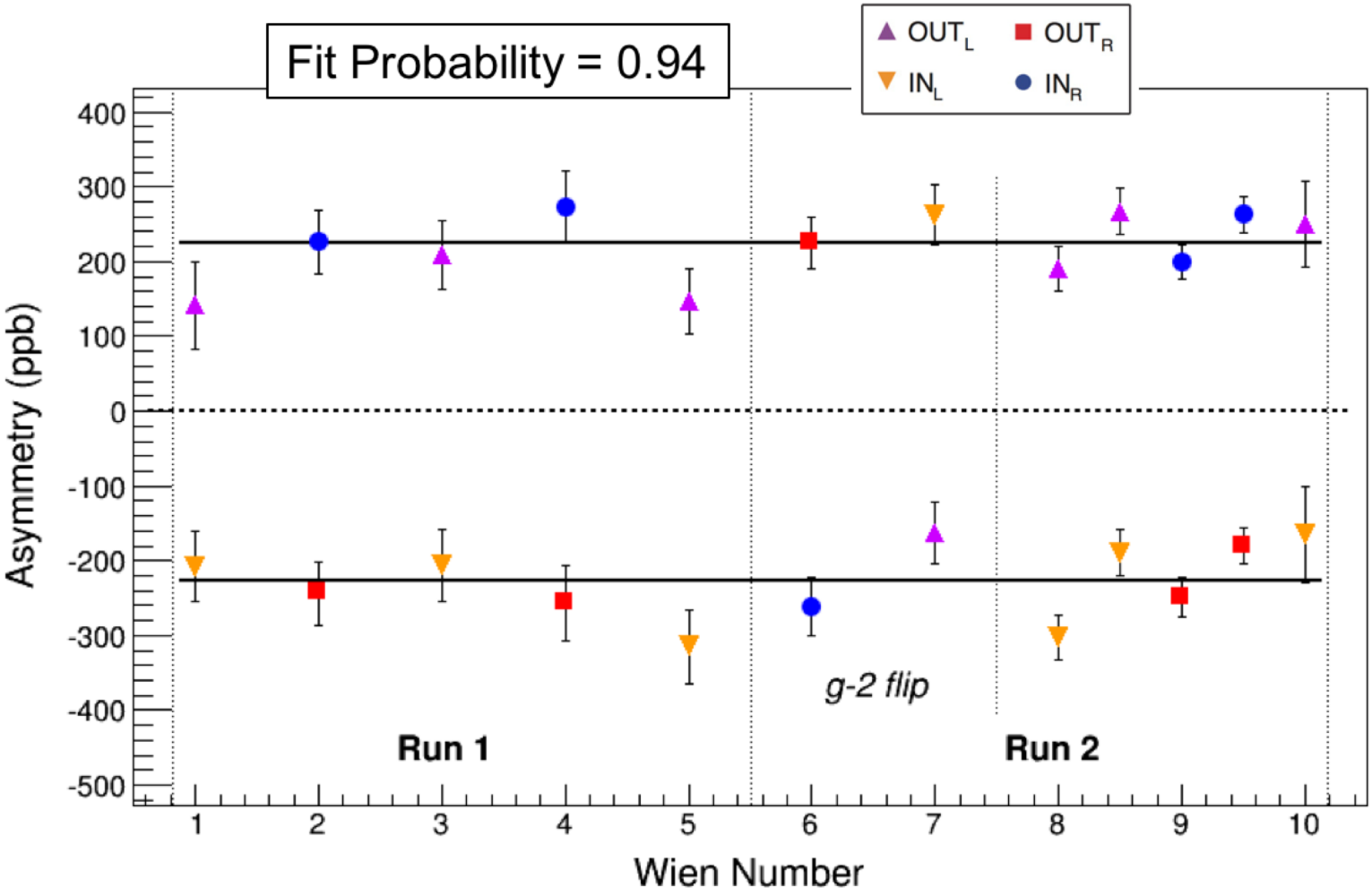

Three slow reversal types:

IN/OUT: reversal of laser helicity (IWHP)

L/R: reversal of electron beam via Wien filter

g-2 flip: reversal of electron via spin precession in accelerator

The data behaved as expected under all three types of slow helicity reversal.

Combining the data without sign corrections gives

NULL average = -1.75 ± 6.51 ppb

- consistent with zero, as expected

Blinded Analysis

Run 1 and 2 *each* had their own independent "blinding factor"
(additive offset in range ± 60 ppb) to avoid analysis bias.

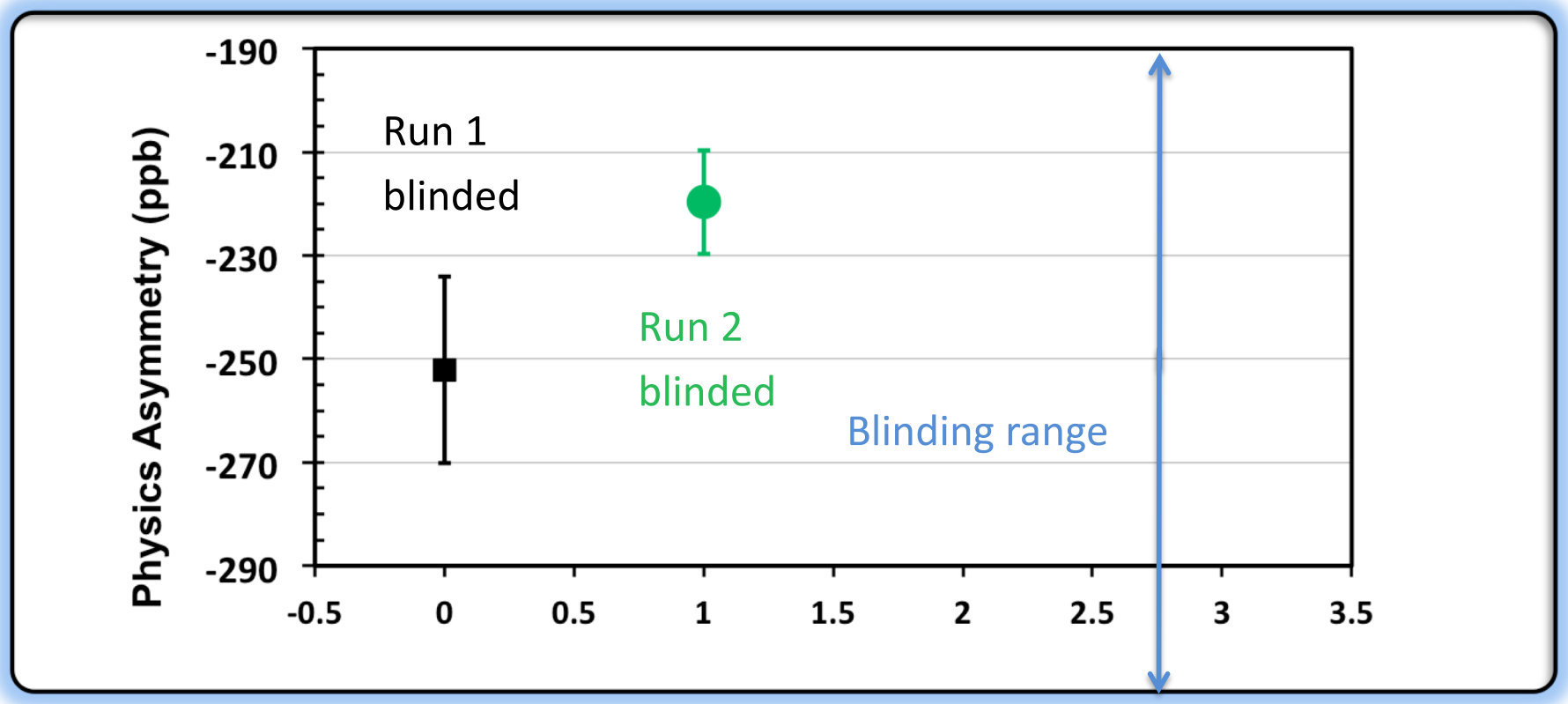

Un-Blinded Results

Marvelous agreement between the two Runs
(several systematic corrections rather different in the two Runs)

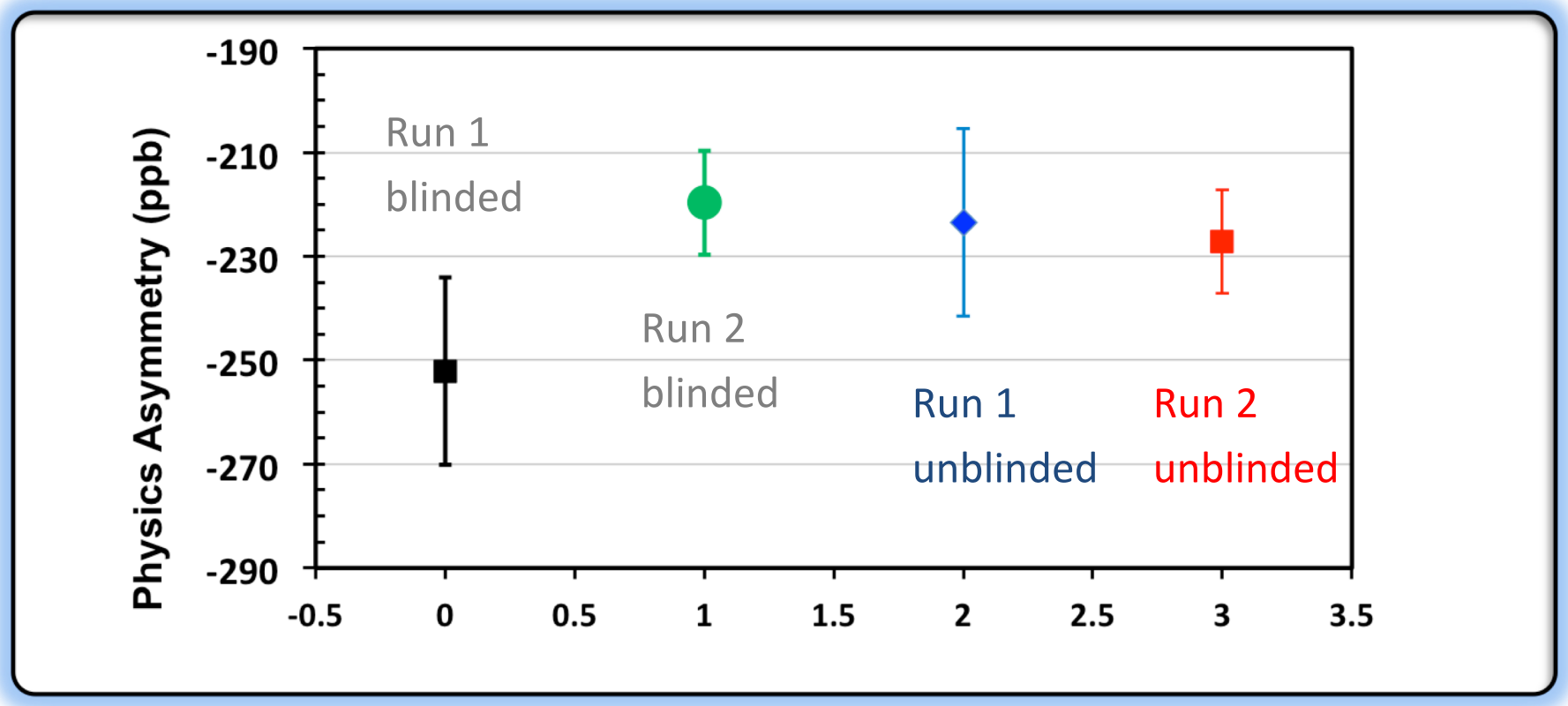

Period	Asymmetry (ppb)	Stat. Unc. (ppb)	Syst. Unc. (ppb)	Tot. Uncertainty (ppb)
Run 1	-223.5	15.0	10.1	18.0
Run 2	-227.2	8.3	5.6	10.0
Run 1 and 2 combined with correlations	-226.5	7.3	5.8	9.3

Extracting Weak Charge from Asymmetry Result

$$A_{ep} = -226.5 \pm 7.3(\text{stat}) \pm 5.8(\text{syst}) \text{ ppb at } \langle Q^2 \rangle = 0.0249 \ (\text{GeV}/c)^2$$

Global fit of world PVES data up to Q^2 = 0.63 GeV^2 to extract proton's weak charge:

$$A_{ep}/A_0 = Q_W^p + Q^2 B(Q^2, \theta), \qquad A_0 = \left[\frac{-G_F Q^2}{4\pi\alpha\sqrt{2}}\right].$$

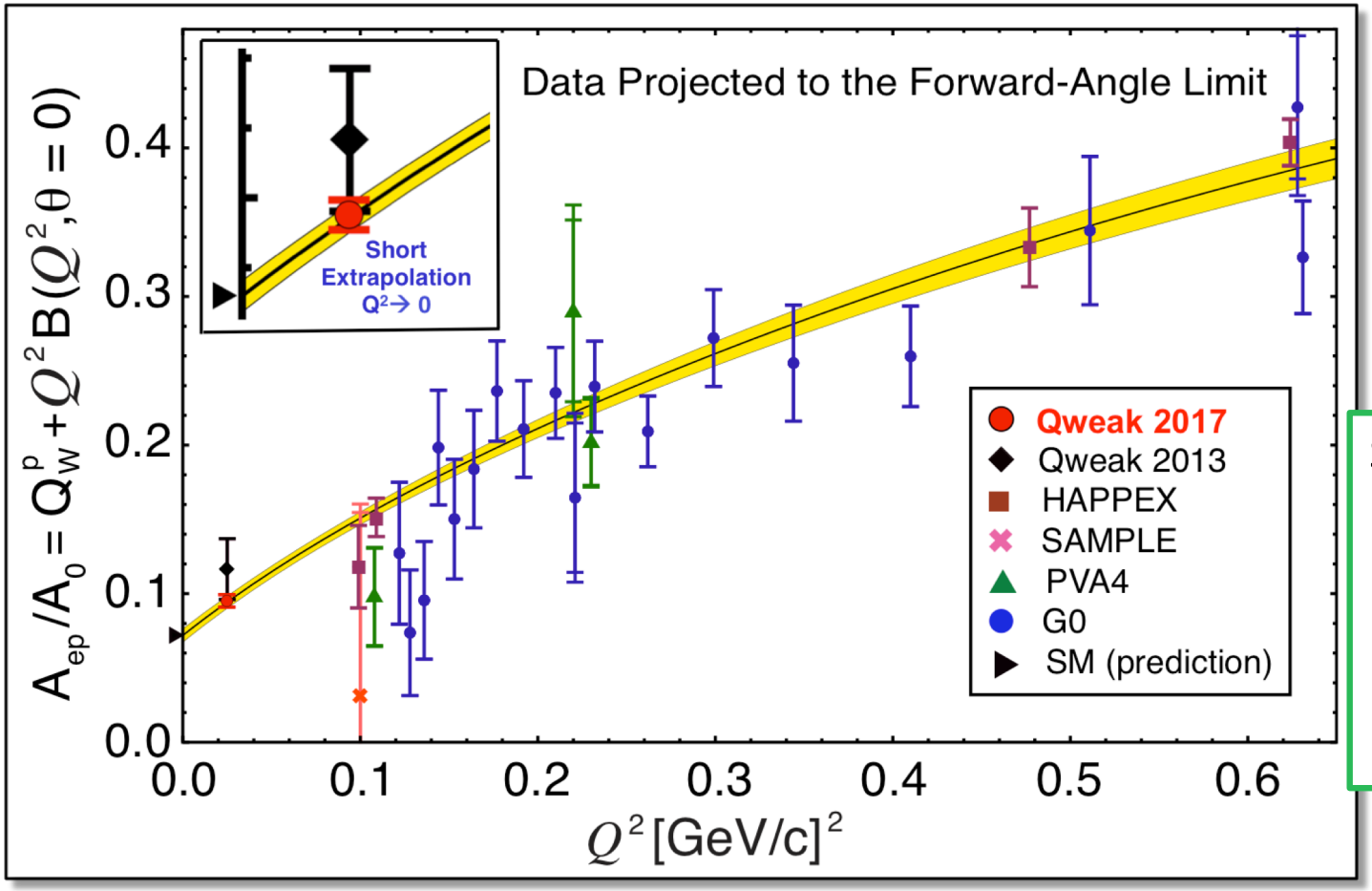

33 entries in PVES (e-p, e-d, e-^{4}He) database

Standard Model:

$$Q_W^p = 0.0708 \pm 0.0003$$

Experiment:

$$Q_W^p = 0.0719 \pm 0.0045$$

Summary of Results from QWeak

Including ^{133}Cs APV result allows extraction of neutron weak charge & separation of C_{1u} , C_{1d} quark coupling constants

Quantity	Value	Error	Method
Q_W^p	0.0719	0.0045	
$\sin^2\theta_W$	0.2382	0.0011	Qweak A_{ep} + PVES data base
ρ_s	0.19	0.11	
μ_s	-0.18	0.15	
$G_A^{Z(T=1)}$	-0.67	0.33	
Q_W^p	0.0718	0.0045	
Q_W^n	**-0.9808**	**0.0063**	Qweak A_{ep} + PVES data base + APV ^{133}Cs
C_{1u}	-0.1874	0.0022	
C_{1d}	0.3389	0.0025	
C_1 correlation = -0.9317			
Q_W^p	0.0684	0.0039	Qweak A_{ep} + PVES data base + LQCD (strange)
$\sin^2\theta_W$	0.2392	0.0009	
Q_W^p	0.0706	0.0047	Qweak A_{ep} + EMFF's & theory axial + LQCD (strange)

Summary of Results from QWeak

Addition of Lattice QCD constraint on strange quarks further improves precision of Q_W^p **&** $\sin^2\theta_W$

Quantity	Value	Error	Method
Q_W^p	0.0719	0.0045	
$\sin^2\theta_W$	0.2382	0.0011	Qweak A_{ep} + PVES data base
ρ_s	0.19	0.11	
μ_s	-0.18	0.15	
$G_A^{Z(T=1)}$	-0.67	0.33	
Q_W^p	0.0718	0.0045	
Q_W^n	-0.9808	0.0063	Qweak A_{ep} + PVES data base + APV ^{133}Cs
C_{1u}	-0.1874	0.0022	
C_{1d}	0.3389	0.0025	
C_1 correlation = -0.9317			
Q_W^p	0.0684	0.0039	Qweak A_{ep} + PVES data base + LQCD (strange)
$\sin^2\theta_W$	0.2392	0.0009	
Q_W^p	0.0706	0.0047	Qweak A_{ep} + EMFF's & theory axial + LQCD (strange)

Summary of Results from QWeak

Addition of Lattice QCD constraint on strange quarks further improves precision of Q_W^p **&** $\sin^2\theta_W$

Quantity	Value	Error	Method
			eak A ep + data base
			eak A ep + data base + ^{133}Cs
			LQCD (strange)

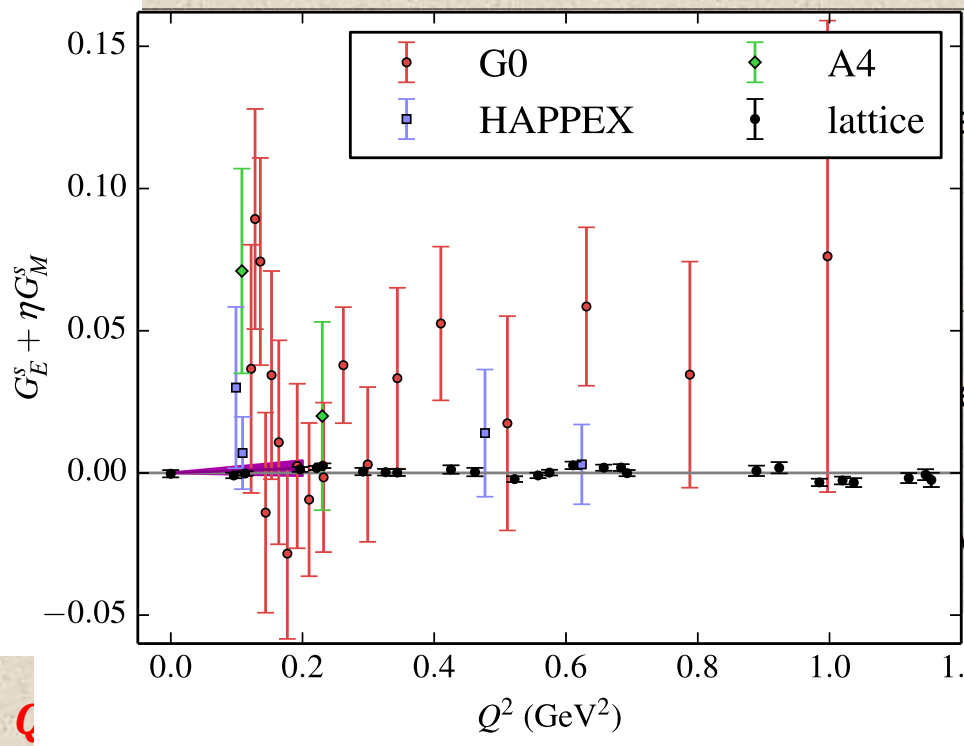

PHYSICAL REVIEW D **92,** 031501(R) (2015)

High-precision calculation of the strange nucleon electromagnetic form factors

Jeremy Green,[1,*] Stefan Meinel,[2,3,†] Michael Engelhardt,[4] Stefan Krieg,[5,6] Jesse Laeuchli,[7] John Negele,[8] Kostas Orginos,[9,10] Andrew Pochinsky,[8] and Sergey Syritsyn[3]

Summary of Results from QWeak

Precision of A_{ep} dominates determination of Q_W^p

Alternate "Standalone" technique to extract Q_W^p does NOT depend on other PV measurements

Quantity	Value	Error	Method
Q_W^p	0.0719	0.0045	
$\sin^2\theta_W$	0.2382	0.0011	Qweak A_{ep} + PVES data base
ρ_s	0.19	0.11	
μ_s	-0.18	0.15	
$G_A^{Z(T=1)}$	-0.67	0.33	
Q_W^p	0.0718	0.0045	
Q_W^n	-0.9808	0.0063	Qweak A_{ep} + PVES data base + APV ^{133}Cs
C_{1u}	-0.1874	0.0022	
C_{1d}	0.3389	0.0025	
C_1 correlation = -0.9317			
Q_W^p	0.0684	0.0039	Qweak A_{ep} + PVES data base + LQCD (strange)
$\sin^2\theta_W$	0.2392	0.0009	
Q_W^p	0.0706	0.0047	Qweak A_{ep} + EMFF's & theory axial + LQCD (strange)

Electroweak Radiative Corrections

In the Standard Model, the weak charge is *defined* at $Q^2 = 0, E = 0$.

$$Q_W^p = [\rho_{NC} + \Delta_e][1 - 4\sin^2\hat{\theta}_W(0) + \Delta_e'] + \square_{WW} + \square_{ZZ} + \square_{\gamma Z}$$

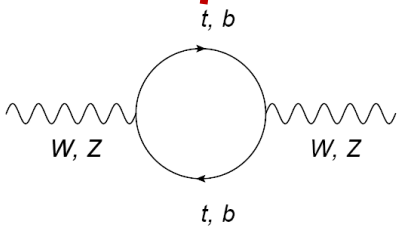

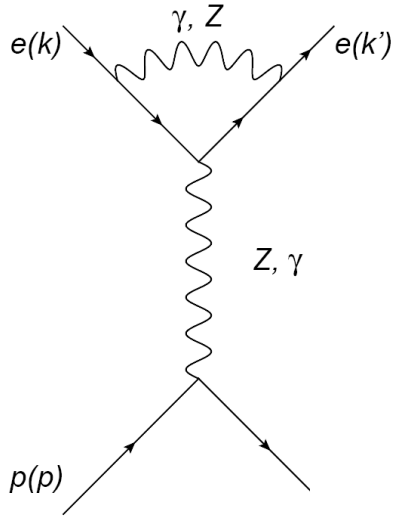

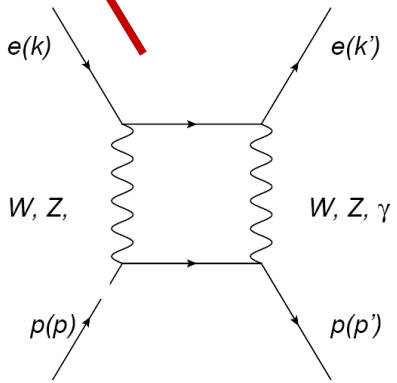

Full expression for Q_W^p has energy dependent corrections – need precise calculations

The $\square_{WW}$ and $\square_{ZZ}$ are well determined from pQCD ($\propto \frac{1}{q^2 - M_{W(Z)}^2 + i\epsilon}$)

The $\square_{\gamma Z}$ isn't pQCD friendly due to the photon leg ($\propto \frac{1}{q^2 + i\varepsilon}$)

Electroweak Radiative Corrections

$$Q_W^p = (1 + \Delta\rho + \Delta_e)\left(1 - 4\sin^2\theta_W(0) + \Delta_e'\right) + \Box_{WW} + \Box_{ZZ} + \Box_{\gamma Z}(0)$$

Term	Expression	Value
ρ_{NC}	$1 + \Delta_\rho$	1.00066
Δ_e	$-\alpha/2\pi$	−0.001161
Δ_e'	$-\frac{\alpha}{3\pi}(1 - 4\hat{s}^2)\left[\ln\left(\frac{M_Z^2}{m_e^2}\right) + \frac{1}{6}\right]$	−0.001411
$\hat{\alpha}$	$\equiv \alpha(M_Z)$	1/127.95
$\hat{s}^2$	$= 1 - \hat{c}^2 \equiv \sin^2\theta_W(M_Z)$	0.23129
$\alpha_s(M_W^2)$	-	0.12072
$\Box_{WW}$	$\frac{\hat{\alpha}}{4\pi\hat{s}^2}\left[2 + 5\left(1 - \frac{\alpha_s(M_W^2)}{\pi}\right)\right]$	0.01831
$\Box_{ZZ}$	$\frac{\hat{\alpha}}{4\pi\hat{s}^2\hat{c}^2}\left[9/4 - 5\hat{s}^2\right]\left(1 - 4\hat{s}^2 + 8\hat{s}^2\right)\left(1 - \frac{\alpha_s(M_Z^2)}{\pi}\right)$	0.00185
$\Box_{\gamma Z}$	axial-vector hadron piece of $\Box_{\gamma Z}$: $\Re\mathrm{e}\,\Box_{\gamma Z}^{\mathrm{A}}$	0.0044

Calculations of the $\Box^{V}_{\gamma Z}$ @ E=1.16 GeV

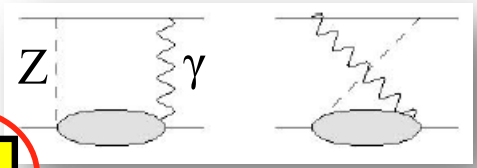

$$Q_W^p = [\rho_{\mathrm{NC}} + \Delta_e][1 - 4\sin^2\hat{\theta}_{\mathrm{W}}(0) + \Delta_e'] + \Box_{WW} + \Box_{ZZ} + \Box_{\gamma Z}$$

The $\Box_{\gamma Z}$ is the only E & Q^2 dependent EW correction.
→ Correct the PVES data for this E & Q^2 dependence.

- Early calculations primarily dispersion theory type
  - Data can firm up error estimates!
  - Qweak: inelastic asymmetry data taken at W ~ 2.3 GeV, Q^2 = 0.09 GeV^2

Gamma-Z Box Error:
AJM-II: Hall et al. (2016)

	Value	Error
V	0.0054	0.0004
AV	-0.0007	0.0002
Q factor	0.978	0.012
(A+V)Q	0.00460	0.00044
Qw(p) SM	0.07080	0.00030

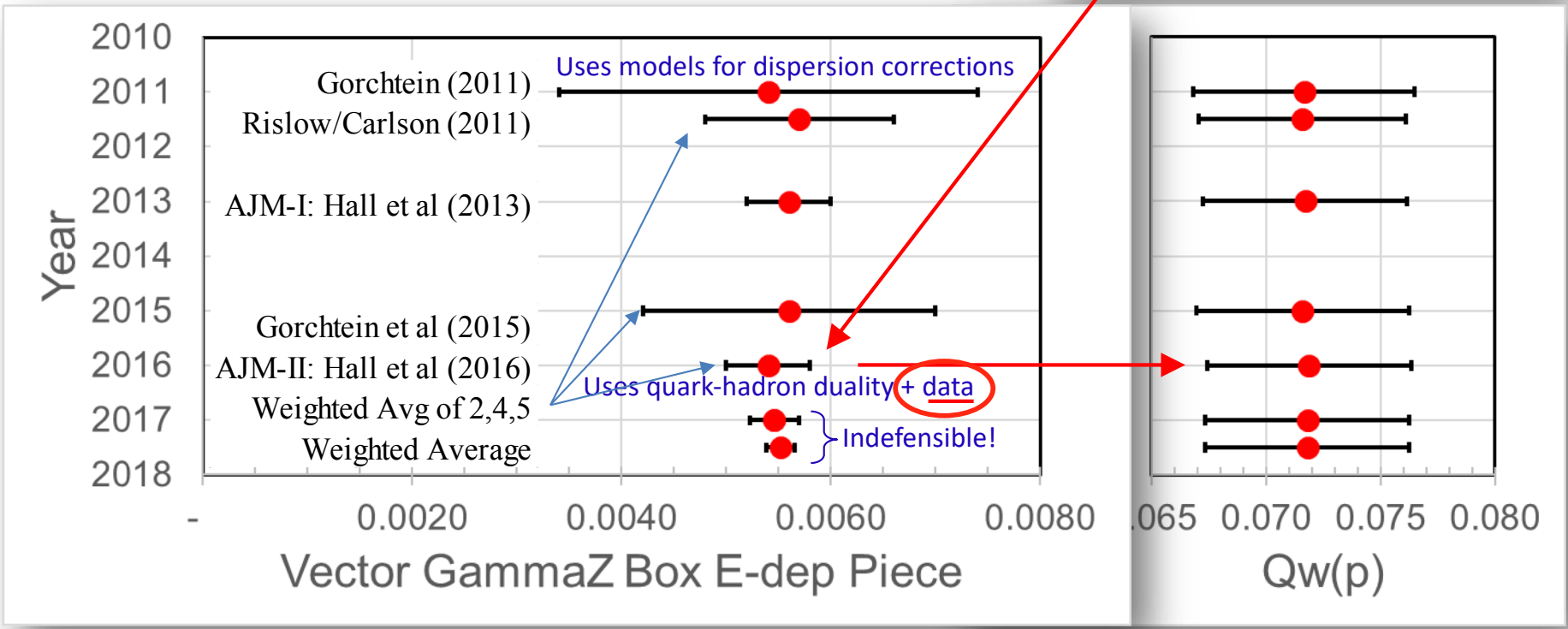

Parity-Violation in DIS region from Qweak

Preliminary Result

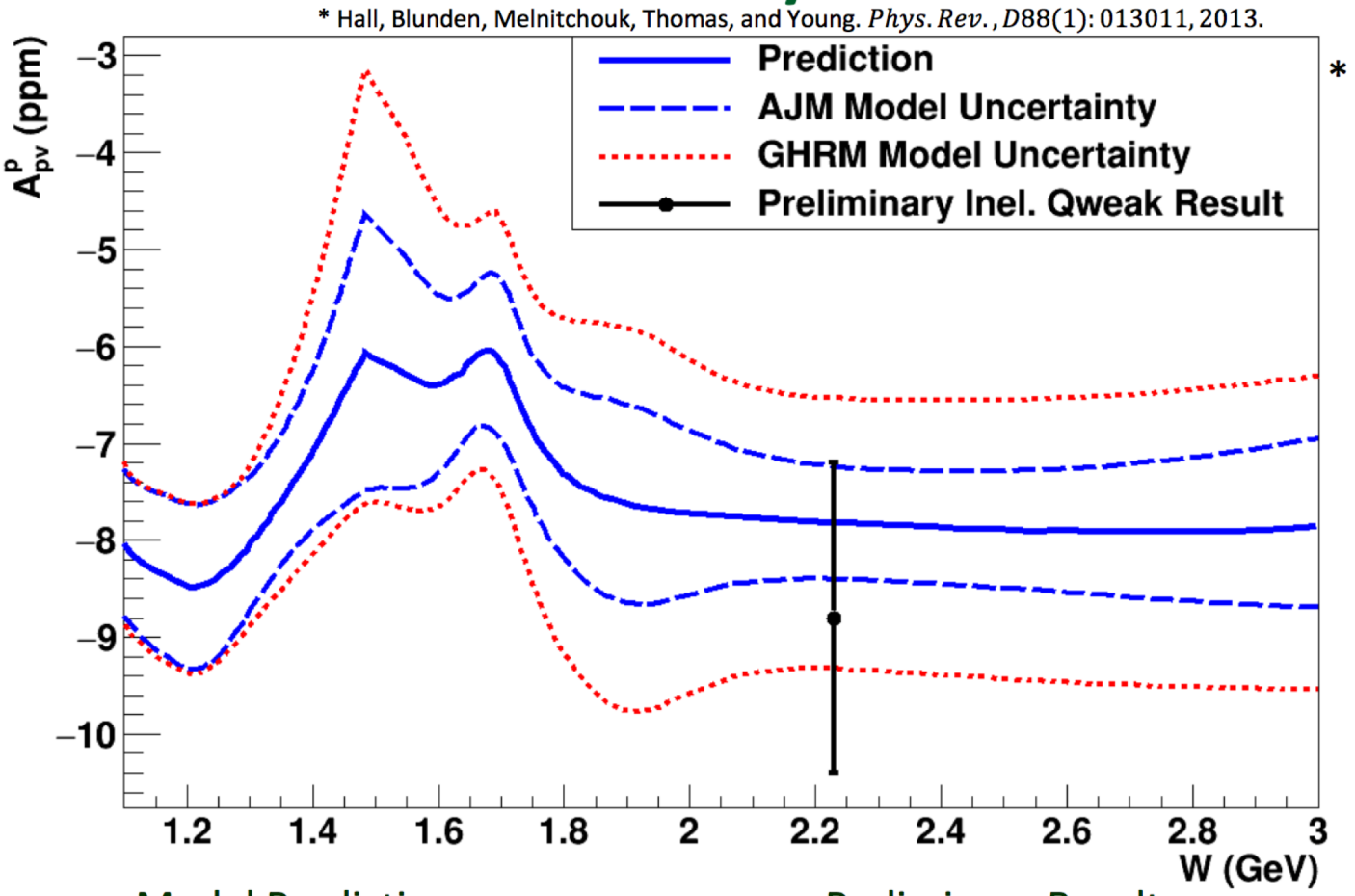

Model Predictions

$Q^2 = 0.09\ GeV^2$

$A^p_{PV} = -7.8 \pm 0.6$ ppm

$A^p_{PV} \approx -7.8 \pm 1.2$ ppm

Preliminary Result

$Q^2 = 0.075\ GeV^2$

$A_{phys} = -8.8 \pm 0.9(stat) \pm 1.3(syst)$ ppm

Electroweak Radiative Corrections

Q_W^p expt. precision : ± 0.0045

$$Q_W^p = (1 + \Delta\rho + \Delta_e)\left(1 - 4\sin^2\theta_W(0) + \Delta_e'\right) + \Box_{WW} + \Box_{ZZ} + \Box_{\gamma Z}(0)$$

Correction to Q_W^p	Uncertainty
$\Delta \sin^2\theta_W(M_Z)$	± 0.0006
$\Box_{WW}, \Box_{ZZ}$ - pQCD	± 0.0003
$\Delta\rho$ (hadronic loops)	± 0.0003
$\Box_{\gamma Z}$	0.00459 ± 0.00044

Erler, Kurylov & Ramsey-Musolf PRD **68**, 016006 (2008)

Calculation	$\Box_{\gamma Z}$ (vector) contribution to Q_W^p
Sibirtsev, Blunden, Melnitchouk & Thomas PRC **82**, 013011 (2010)	$0.0047^{+0.0011}_{-0.0004}$
Rislow & Carlson PRD **83**, 113007 (2011)	0.0057 ± 0.0009
Gorchtein, Horowitz & Ramsey-Musolf PRC **84**, 015502 (2011)	0.0054 ± 0.0020
Hall, Blunden, Melnitcouk, Thomas & Young Phys.Lett.B **753**, 221 (2016)	0.0052 ± 0.00043

Running of the Weak Mixing angle $\sin^2\theta_W$

$$Q_W^p = 1 - 4\sin^2\theta_W \approx 0$$

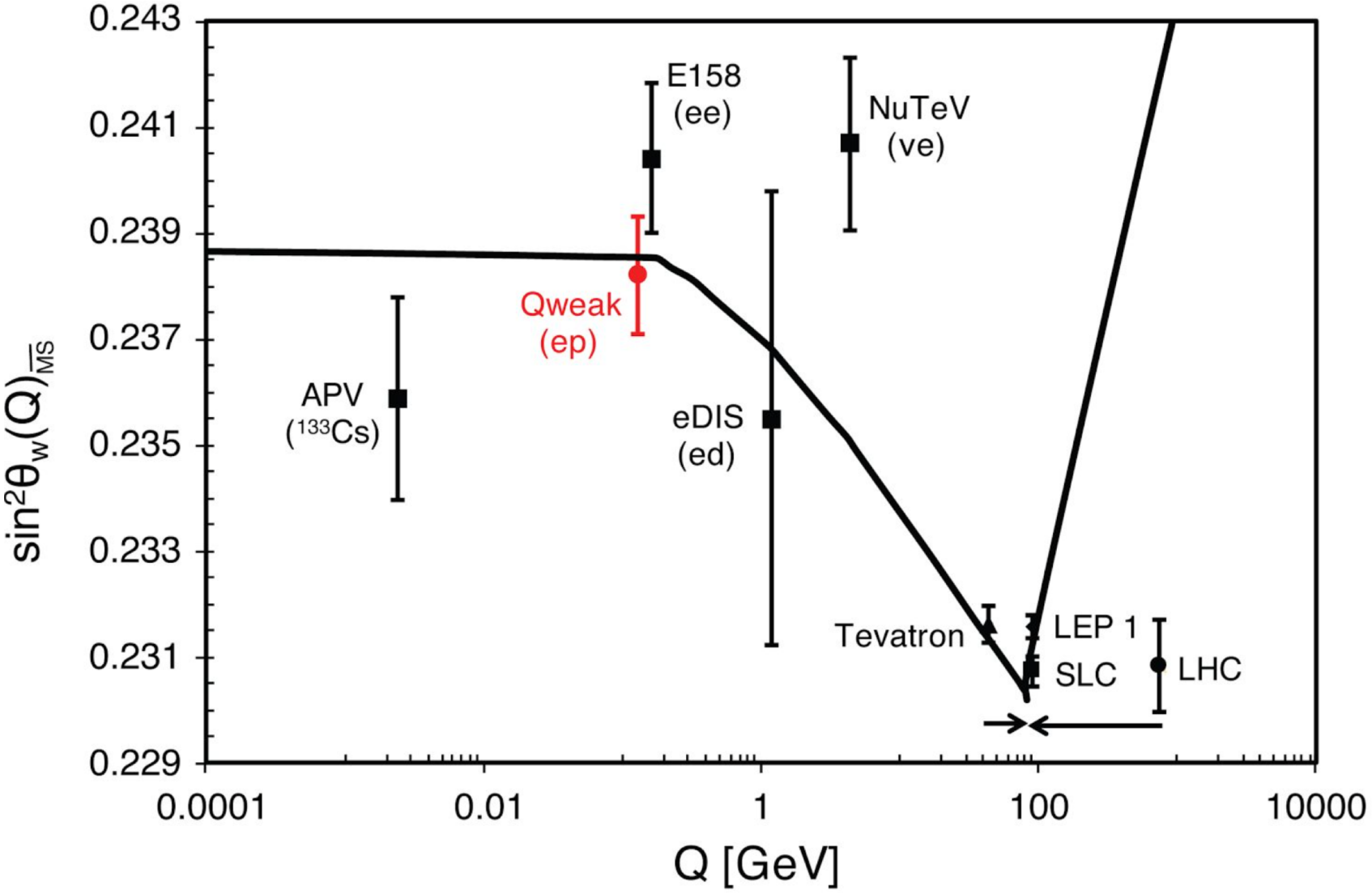

Solid Curve:
J. Erler, M. Ramsey-Musolf, P. Langacker

Note: interference effects of heavy new physics (*i.e.* Z', leptoquarks) suppressed at Z resonance → LEP/SLC mass limits $\lesssim$ TeV, while low energy observables probe few TeV scale

Sensitivity to New Physics at TeV scale

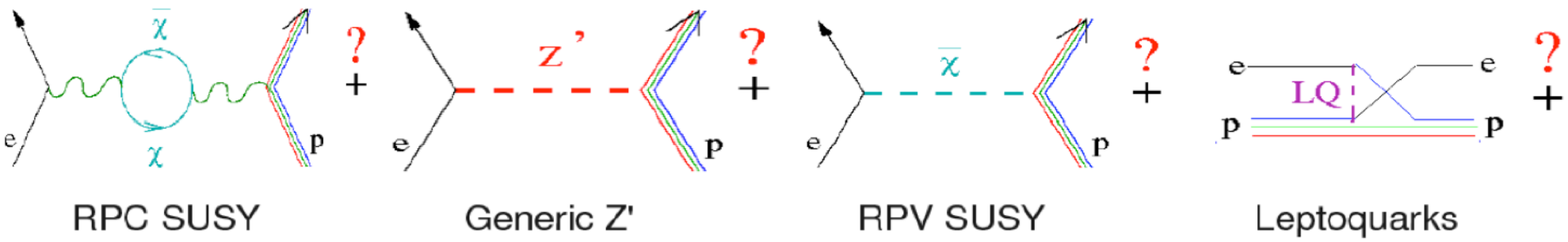

Parameterize generically by adding contact term to Lagrangian:

$$\mathcal{L}^{\text{eq}}_{\text{NC}} = -\frac{G_F}{\sqrt{2}}\bar{e}\gamma_\mu\gamma_5 e\sum_q C_{1q}\bar{q}\gamma^\mu q.$$

Standard Model term

$$\mathcal{L}^{\text{PV}}_{\text{NP}} = -\frac{g^2}{4\Lambda^2}\bar{e}\gamma_\mu\gamma_5 e\sum_q h_V^q\bar{q}\gamma^\mu q$$

New Physics term

g=coupling
Λ=mass scale

Limits on Semi-Leptonic PV Physics beyond the SM

$$Q_W^p = -2(2C_{1u} + C_{1d})$$

New Physics Ruled Out
@95% CL Below Mass Scale of Λ/g

$$\mathcal{L}_{\mathrm{NP}}^{\mathrm{PV}} = -\frac{g^2}{\Lambda^2}\bar{e}\gamma_\mu\gamma_5 e \sum_q h_V^q \bar{q}\gamma^\mu q$$

$$h_V^u = \cos\theta_h \qquad h_V^d = \sin\theta_h$$

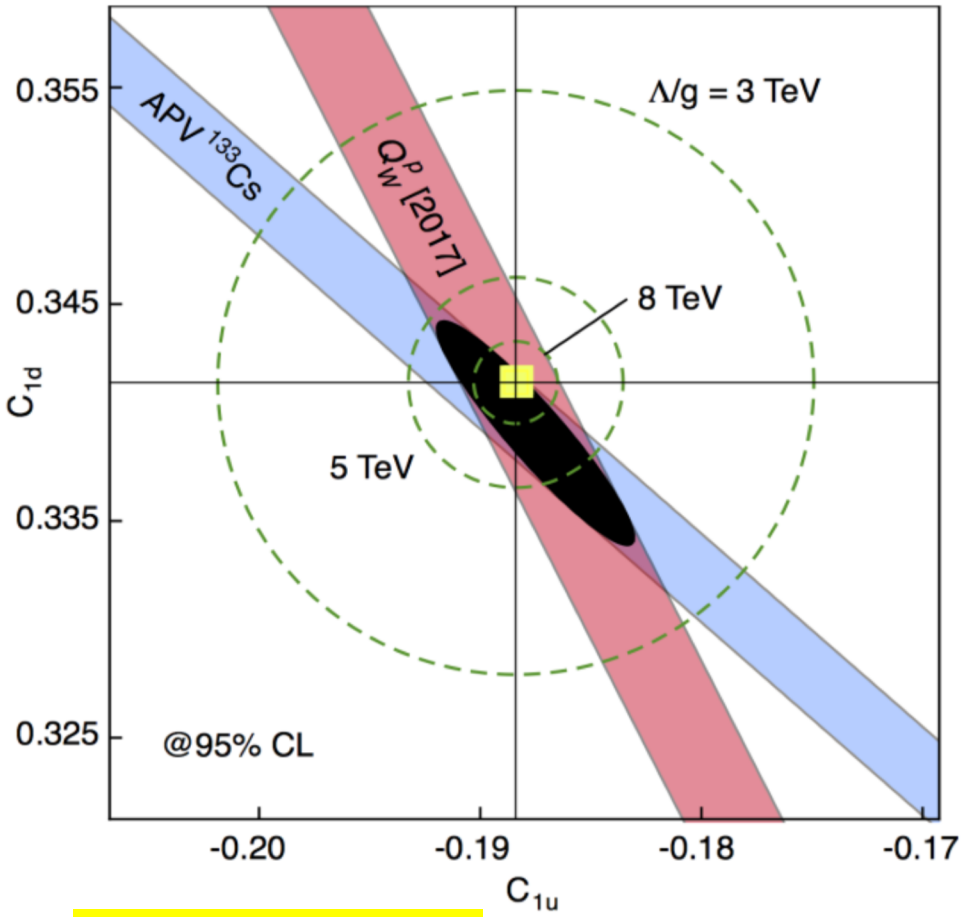

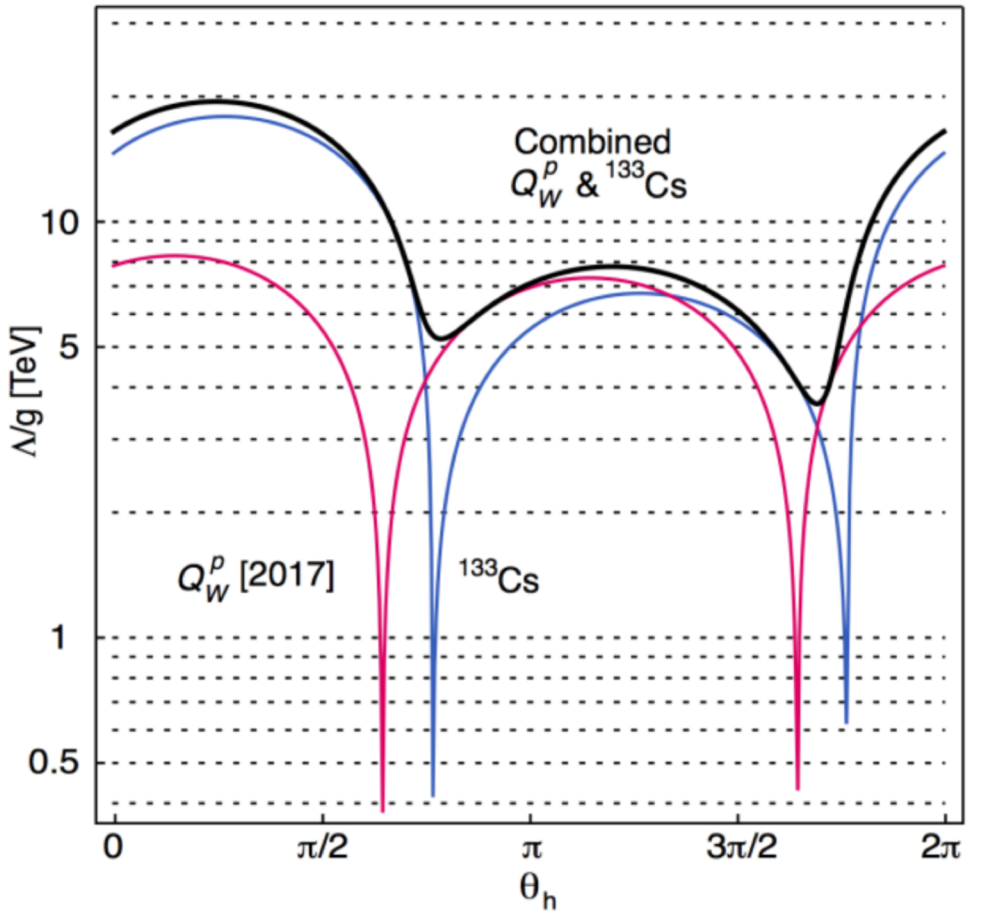

Yellow box: SM values

APV: atomic parity violation ^{133}Cs C.S. Wood et al. Science **275**, 1759 (1997); Dzuba et al. PRL **109**, 203003 (2012)

Example: Implications for Leptoquarks

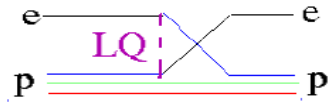

Leptoquarks

- Impact on $Q_W(p)$ of leptoquarks studied by Erler, Kurylov, Ramsey-Musolf, Phys. Rev. D **68**, 016006 (2003)
- Analysis dated (2003), but suggestive; included HERA, LEP, and APV data (missing more recent HERA data: see Aaron, et al. Phys. Lett. B **705**, 52 (2011).)

New Q_{weak} data (6.2% 1σ error) has sensitivity to distinguish among LQ types at 95% CL

Scalar Leptoquarks			Vector Leptoquarks		
LQ	Consistency	$\Delta Q_W(p)/Q_W(p)$	LQ	Consistency	$\Delta Q_W(p)/Q_W(p)$
S_1^L	0.57	9%	$U_{1\mu}^L$	0.26	−8%
S_1^R	0.01	−6%	$U_{1\mu}^R$	0.56	6%
$\tilde{S}_1^R$	0.44	−6%	$\tilde{U}_{1\mu}^R$	0.99	25%
S_3	0.76	10%	$U_{3\mu}$	0.31	−4%
R_2^L	0.44	−13%	$V_{2\mu}^L$	0.87	9%
R_2^R	0.89	15%	$V_{2\mu}^R$	0.11	−7%
$\tilde{R}_2^L$	0.13	−4%	$\tilde{V}_{2\mu}^L$	0.56	14%

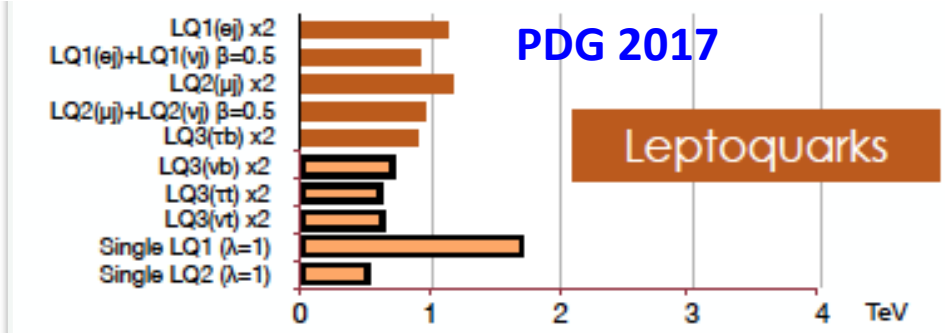

- LHC limits currently at ~ 1 TeV
- Low energy precision data continues to play important role in recent analyses including LHC data: see Phys. Rep. **641**, 1 (2016)

SM tests with Precision Low-Energy Parity Violation

Experiment	% Precision	$\Delta\sin^2\theta_w$	Λ /g [TeV] (mass reach)
SLAC-E122	8.3	0.011	1.5
SLAC-E122	110	0.44	0.25
APV (^{205}Tl)	3.2	0.011	3.8
APV (^{133}Cs)	0.58	0.0019	9.1
SLAC-E158	14	0.0013	4.8
Jlab-Hall A	4.1	0.0051	2.2
Jlab-Hall A	61	0.051	0.82
JLab-Qweak (p)	**6.2**	**0.0011**	**7.5**
JLab-SoLID	0.6	0.00057	6.2
JLab-MOLLER	2.3	0.00026	11.0
Mainz-P2	2.0	0.00036	13.8
APV (^{225}Ra$^+$)	0.5	0.0018	9.6
APV (^{213}Ra$^+$ / ^{225}Ra$^+$)	0.1	0.0037	4.5
PVES (^{12}C)	0.3	0.0007	14

Published

Planned

New Physics at Lower Energy Scales?

QWeak result also sensitive to possible new physics with mass scales well below energy frontier, which may be “hidden” or hard to access at colliders (long as it is parity-violating).

Example: Implications for "Dark Parity Violation"

"Dark Z" – possible portal for new force to communicate with SM?

(Davoudiasl, Lee, Marciano, Phys. Rev. D**89**, 095006 (2014), & Marciano (private communication)

- New source of low-energy PV through mass mixing between Z_0 and Z_d
- Sensitivity is at low Q, not Z-pole
- Complementary to direct searches for heavy dark photons
  - observable even if direct decay modes are "invisible"
- **New Q_{weak} point rules out some of the allowed region**

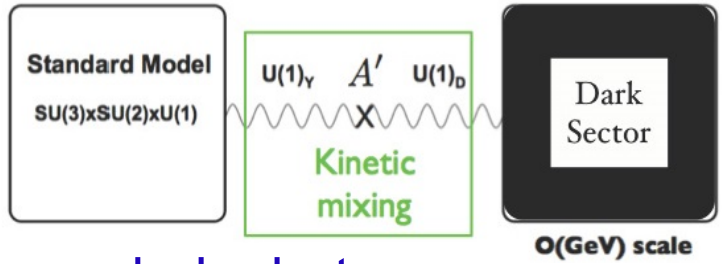

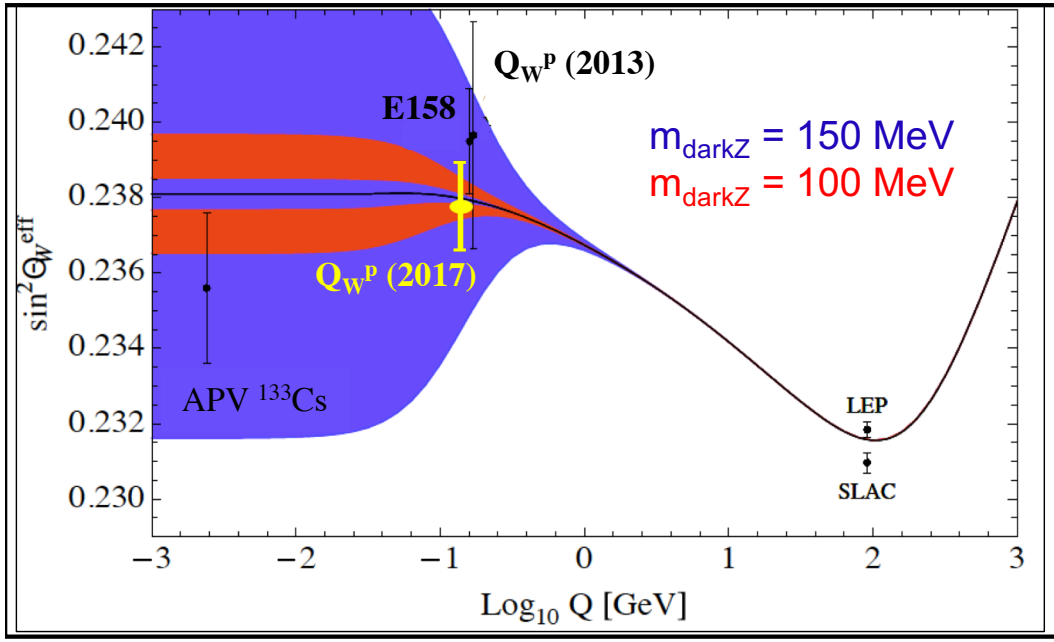

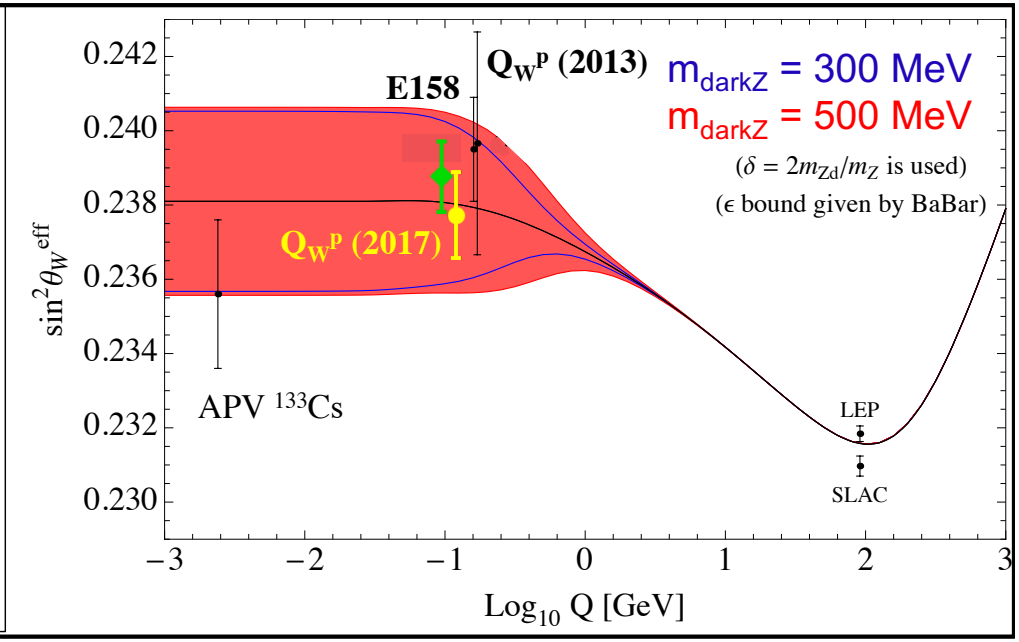

A suite of Auxiliary Measurements

Many ancillary measurements done to quantify various systematic effects:

Q_{weak} has data (under analysis) on a variety of observables of interest for hadronic physics:

Beam normal single-spin asymmetry* (BNSSA) for elastic scattering on proton
BNSSA for elastic scattering on ^{12}C, ^{27}Al
PV asymmetry in the $N \rightarrow \Delta$ region.
BNSAA in the $N \rightarrow \Delta$ region.
BNSSA near W= 2.5 GeV
BNSSA in pion photoproduction
PV asymmetry in inelastic region near W=2.5 GeV (related to γZbox diagrams)
PV asymmetry for elastic from ^{27}Al [see W. Deconinck's talk on May 3]
PV asymmetry in pion photoproduction

*: *aka* vector analyzing power *aka* transverse asymmetry;
generated by imaginary part of two-photon exchange amplitude

The QWeak Collaboration

101 collaborators 26 grad students
11 post docs 27 institutions

Institutions:

[1] University of Zagreb
[2] College of William and Mary
[3] A. I. Alikhanyan National Science Laboratory
[4] Massachusetts Institute of Technology
[5] Thomas Jefferson National Accelerator Facility
[6] Ohio University
[7] Christopher Newport University
[8] University of Manitoba,
[9] University of Virginia
[10] TRIUMF
[11] Hampton University
[12] Mississippi State University
[13] Virginia Polytechnic Institute & State Univ
[14] Southern University at New Orleans
[15] Idaho State University
[16] Louisiana Tech University
[17] University of Connecticut
[18] University of Northern British Columbia
[19] University of Winnipeg
[20] George Washington University
[21] University of New Hampshire
[22] Hendrix College, Conway
[23] University of Adelaide
[24] Syracuse University
[25] Duquesne University

A SEARCH FOR NEW PHYSICS
Qweak

D. Androic,[1] D.S. Armstrong,[2] A. Asaturyan,[3] T. Averett,[2] J. Balewski,[4] K. Bartlett,[2] J. Beaufait,[5] R.S. Beminiwattha,[6] J. Benesch,[5] F. Benmokhtar,[7,25] J. Birchall,[8] R.D. Carlini,[5, 2] G.D. Cates,[9] J.C. Cornejo,[2] S. Covrig,[5] M.M. Dalton,[9] C.A. Davis,[10] W. Deconinck,[2] J. Diefenbach,[11] J.F. Dowd,[2] J.A. Dunne,[12] D. Dutta,[12] W.S. Duvall,[13] M. Elaasar,[14] W.R. Falk*,[8] J.M. Finn*[2],T. Forest,[15, 16], C. Gal,[9] D. Gaskell,[5] M.T.W. Gericke,[8] J. Grames,[5] V.M. Gray,[2] K. Grimm,[16, 2] F. Guo,[4] J.R. Hoskins,[2] K. Johnston,[16] D. Jones,[9] M. Jones,[5] R. Jones,[17] M. Kargiantoulakis,[9] P.M. King,[6] E. Korkmaz,[18] S. Kowalski,[4] J. Leacock,[13] J. Leckey,[2,] A.R. Lee,[13] J.H. Lee,[6, 2,] L. Lee,[10] S. MacEwan,[8] D. Mack,[5] J.A. Magee,[2] R. Mahurin,[8] J. Mammei,[13,] J.W. Martin,[19] M.J. McHugh,[20] D. Meekins,[5] J. Mei,[5] R. Michaels,[5] A. Micherdzinska,[20] A. Mkrtchyan,[3] H. Mkrtchyan,[3] N. Morgan,[13] K.E. Myers,[20] A. Narayan,[12] L.Z. Ndukum,[12] V. Nelyubin,[9] H. Nuhait,[16] Nuruzzaman,[11, 12] W.T.H van Oers,[10, 8] A.K. Opper,[20] S.A. Page,[8] J. Pan,[8] K.D. Paschke,[9] S.K. Phillips,[21] M.L. Pitt,[13] M. Poelker,[5] J.F. Rajotte,[4] W.D. Ramsay,[10, 8] J. Roche,[6] B. Sawatzky,[5] T. Seva,[1] M.H. Shabestari,[12] R. Silwal,[9] N. Simicevic,[16] G.R. Smith,[5] P. Solvignon*,[5] D.T. Spayde,[22] A. Subedi,[12] R. Subedi,[20] R. Suleiman,[5] V. Tadevosyan,[3] W.A. Tobias,[9] V. Tvaskis,[19, 8] B. Waidyawansa,[6] P. Wang,[8] S.P. Wells,[16]S.A. Wood,[5] S. Yang,[2] R.D. Young,[23] P. Zang,[24] and S. Zhamkochyan [3]

Jefferson Lab

Spokespersons Project Manager Grad Students *deceased

Hall C

Summary

Precision measurement of proton's weak charge: $Q_W^p = 0.0719 \pm 0.0045$

Excellent agreement with Standard Model prediction = 0.0708

Constrains generic new parity-violating "Beyond the Standard Model" physics at TeV scale: $\Lambda/g > 3.6$ TeV (arbitrary u/d ratio of couplings)

Result robust against extraction technique

Completes "Weak Charge triad": *(e, n, p)*

Result in-press in *Nature*

Important addition to global electroweak fits to constrain many new physics scenarios

Thanks!

Extra Slides

Asymmetry and Hadronic Form Factors

- $A_{ep} = \left[\frac{\sigma^+ - \sigma^-}{\sigma^+ + \sigma^-}\right] \propto$

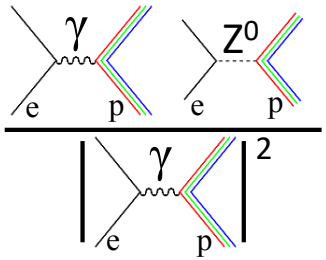

- $A_{ep} = \left[\frac{G_F\, Q^2}{4\pi\alpha\sqrt{2}}\right] \frac{\epsilon G_E^{p\gamma} G_E^{pZ} + \tau G_M^{p\gamma} G_M^{pZ} - (1-4\sin^2\theta_W)\epsilon' G_M^{p\gamma} \overbrace{G_A^Z}^{\text{Axial FF}}}{\varepsilon (G_E^{p\gamma})^2 + \tau (G_M^{p\gamma})^2}$ tree level

  - $G_{E,M}^{pZ} = \underbrace{(1-4\sin^2\theta_W)}_{Q_W^p} \underbrace{G_{E,M}^{p\gamma} - G_{E,M}^{n\gamma}}_{\text{EM FFs}} - \underbrace{G_{E,M}^{s}}_{\text{Strange FF}}$ is the proton's neutral electroweak FF

- Recast: $A_{ep}/A_0 \rightarrow \left[Q_w^p + Q^2 \underbrace{B(Q^2,\theta)}_{\text{hadronic structure (FFs)}}\right]$, where $A_0 = \frac{G_F\, Q^2}{4\pi\alpha\sqrt{2}}$

$$Q_E^s = \rho_s Q^2 G_D \qquad Q_M^s = \mu_s G_D \qquad Q_D = \frac{1}{(1 - Q^2/\Lambda^2)} \qquad \Lambda = 1.0\ \mathrm{GeV}/c$$

$$Q_A^{Z\ (T=1)} = (G_A^p - G_A^n)/2$$

EM FFs : Arrington and Sick
Phys. Rev. C **76**, 035201 (2007).

Transverse Asymmetry Measurement

Normal production running: 89% longitudinal beam polarization

Small amount of transverse polarization

- Large parity conserving asymmetry (~5ppm)
- Leaks into the experimental asymmetry through broken azimuthal symmetry

Measurements of the Beam Normal Single Spin Asymmetry (BNSSA) provide:

- Direct access to imaginary part of two-photon exchange

We need to correct for this…

Horizontal and vertical components measured separately

$$A_{BNSS}(\phi_{det}) = B_n |P_T| \sin(\phi_{det} - \phi_s)$$

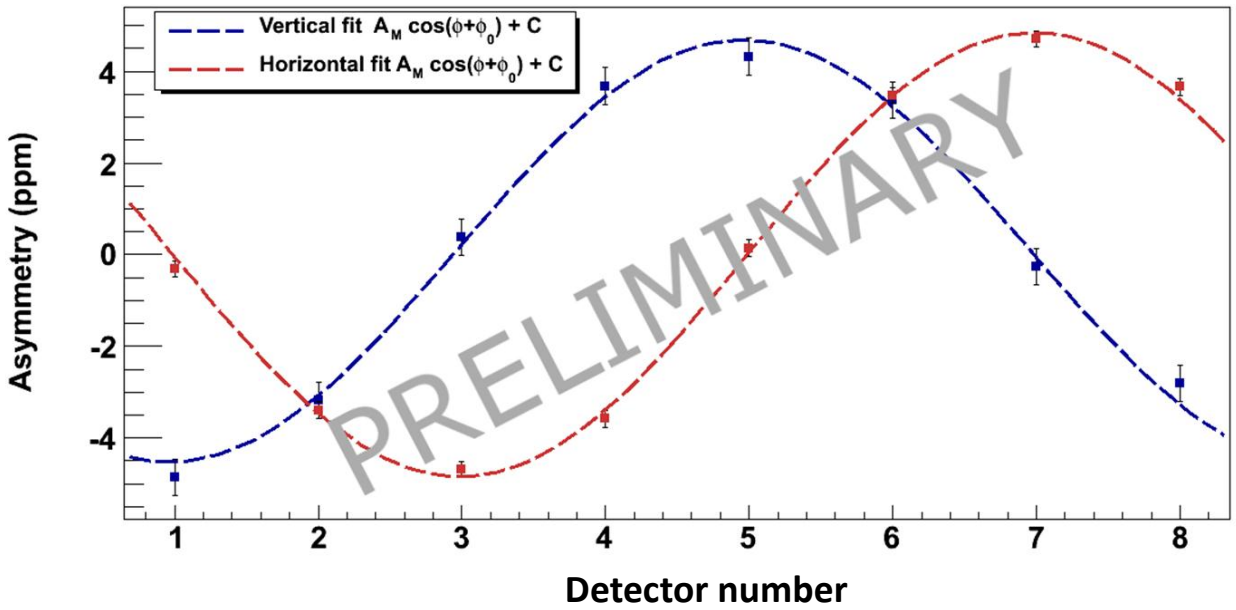

Transverse Asymmetry Measurement

Normal production running: 89% longitudinal beam polarization

Small amount of transverse polarization

- Large parity conserving asymmetry (~5ppm)
- Leaks into the experimental asymmetry through broken azimuthal symmetry

$$B_n = -5.30 \pm 0.07(stat) \pm 0.15(sys) \text{ ppm}$$

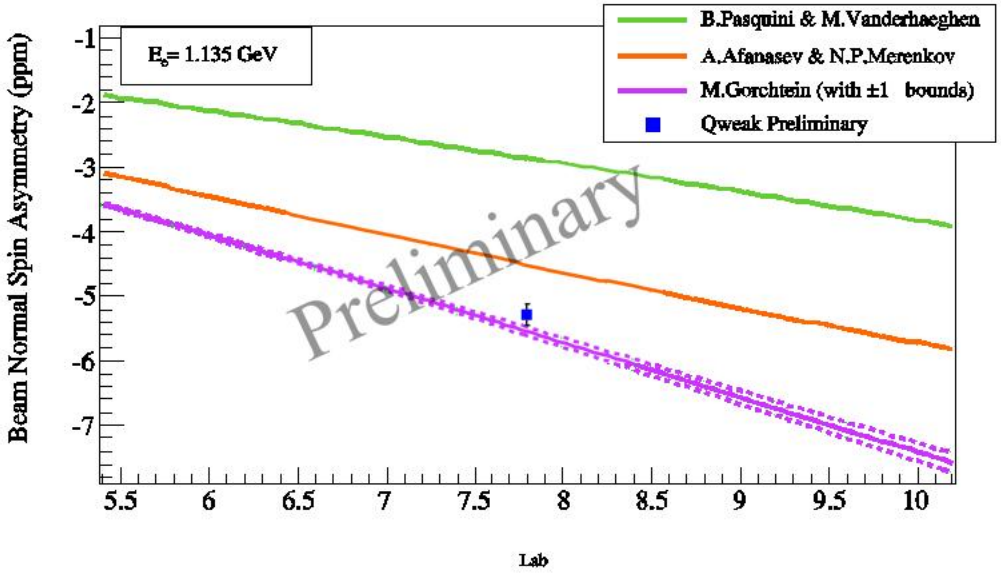

Source	Preliminary	Anticipated
Polarization	2.2%	~1.0%
Statistics	1.3%	~1.3%
Q^2	1.2%	~0.5%
Non-linearity	1.0%	~0.2%
Regression	0.9%	~0.9%
Backgrounds	0.3%	~0.3%

This is the most precise measurement of Beam Normal Single Spin Asymmetry to date.

PhD thesis of Buddhini Waidyawansa; being prepared for publication

$N\rangle$ Δ Parity Violating Asymmetry

Beam Energy	$<\varphi>$	$<Q^2>$	$<W>$ (Missing Mass)
1165 MeV	8.3°	0.021 GeV^2	1205 MeV
877 MeV	8.4°	0.011 GeV^2	1189 MeV

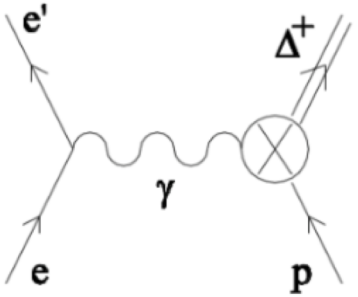

$$\vec{e}^{-} + p \langle \Delta^{+} + e^{-} \langle N + \varphi + e^{-}$$

_EW_meeting

- Allows extraction of low energy constant, d_Δ, related to hadronic parity violation

$$A_{PV}^{\square} \langle \frac{d_\Delta M_N}{\Lambda_X}$$

- Two sets of data gives two values of d_Δ
- Q_{weak} values are centered at $d_\Delta = 0$ to show expected precision

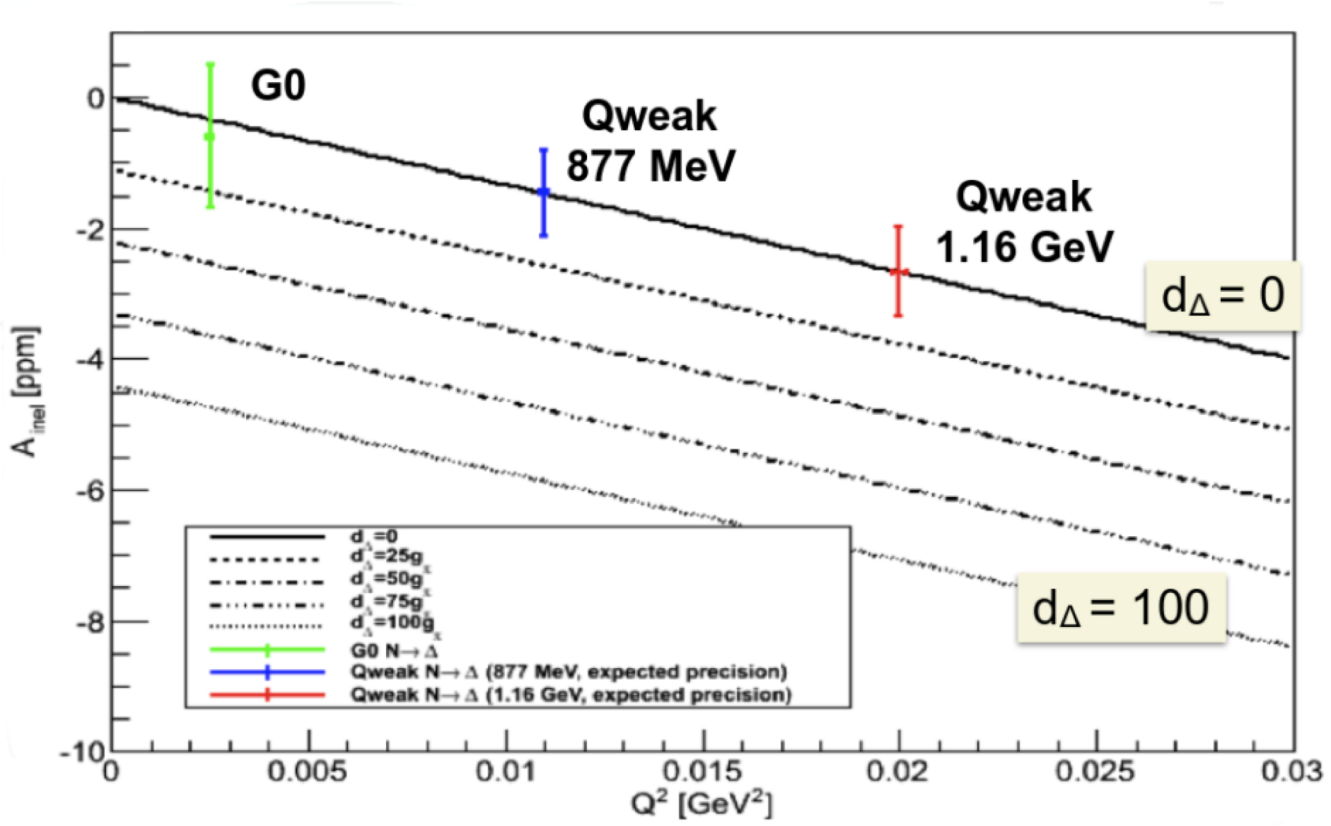

Helicity-Correlated Beam Parameters

- Beam Intensity asymmetry: active (≈ 60 s scale) feedback system (Pockels cell voltage)
- Careful alignment of Pockels cell in source essential:
  → smallest position differences after photocathode yet seen at JLab

- Did not (generally) benefit from "kinematic damping": $X, X' \propto \sqrt{\frac{p_0}{p}}$
  (theoretical reduction factor ~ 60)

- Mis-matched beam transport distorts phase-space ellipse
- One time, we devoted significant time to allow good "matching":
  did see suppression of helicity-correlated differences

Parameter	Max run-averaged HC value	Run1 (Modulation set)	Run2 (Modulation set)
Beam intensity	$\langle A_Q \rangle < 10^{-7}$	-5.0 ± 2.9 (10^{-8})	2.8 ± 1.4 (10^{-8})
Beam energy	$\langle \Delta E/E \rangle \leq 10^{-9}$	-2.0 ± 0.3 (10^{-9})	0.36 ± 0.18 (10^{-9})
Beam position	$\langle \Delta X \rangle < 2$ nm	1.6 ± 1.2 nm	2.2 ± 0.9 nm
	$\langle \Delta Y \rangle < 2$ nm	-6.3 ± 0.9 nm	0.2 ± 0.4 nm
Beam angle	$\langle \Delta\theta_X \rangle < 30$ nrad	-0.15 ± 0.04 nrad	-0.05 ± 0.02 nrad
	$\langle \Delta\theta_Y \rangle < 30$ nrad	0.04 ± 0.04 nrad	-0.05 ± 0.01 nrad

Helicity-Corrector Magnets

- Set of fast pulsed magnets (5 MeV region of injector)
- Kick beam trajectory with helicity (position and angle)
- Measured response at target: stable, as long as accelerator tune unchanged
- “grad student feedback” (daily)

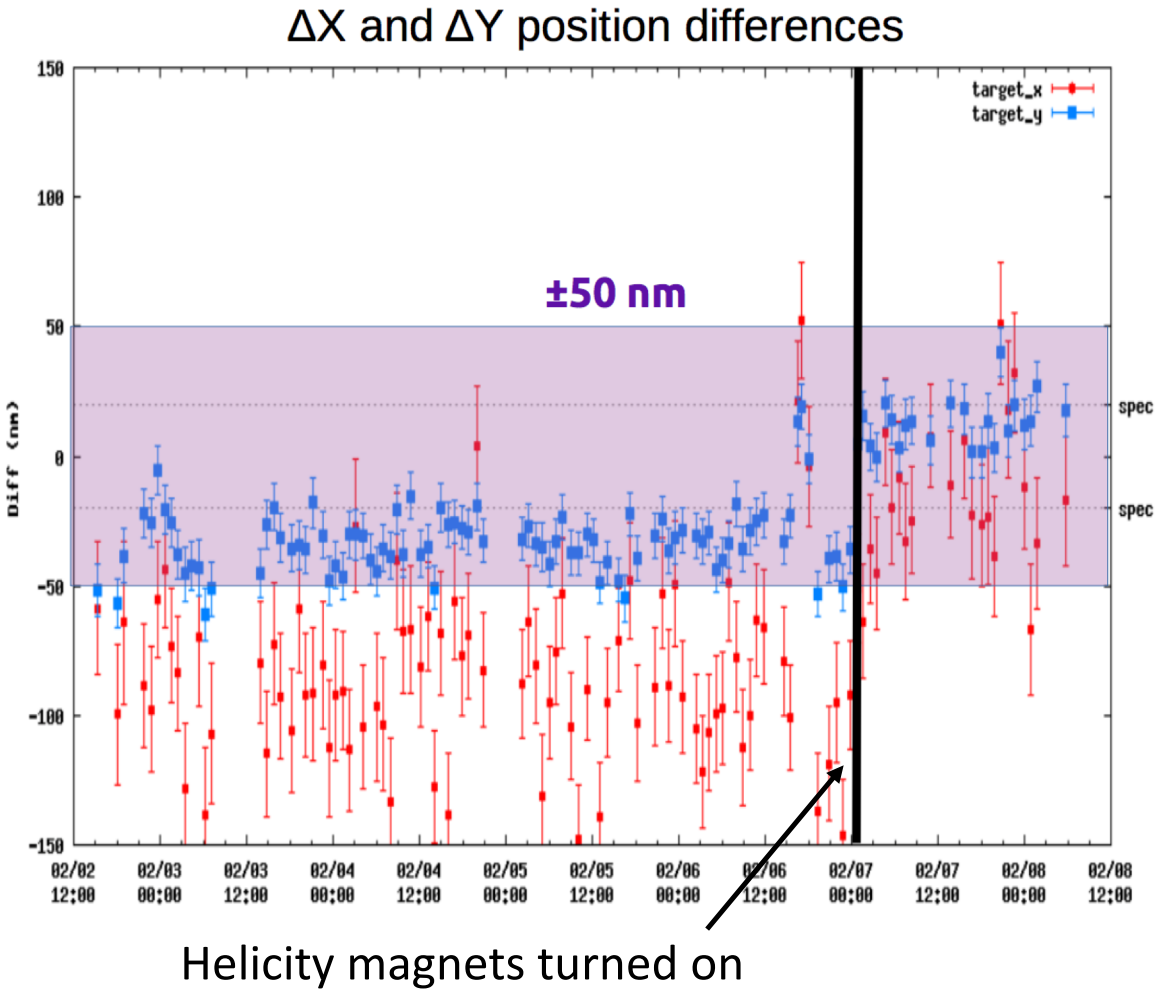

No need for different size kicks for different IWHP (slow flip) states:
Good setup of polarized source

Helicity magnets used for much of our 2nd run.

$N \rangle \Delta$ Parity Violating Asymmetry

Beam Energy	$<\varphi>$	$<Q^2>$	$<W>$ (Missing Mass)
1165 MeV	8.3°	0.021 GeV^2	1205 MeV
877 MeV	8.4°	0.011 GeV^2	1189 MeV

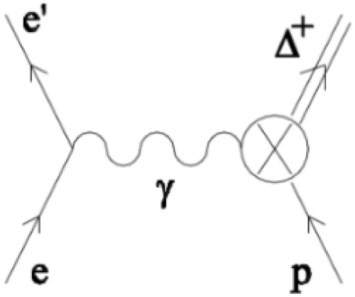

$$\vec{e}^{-} + p \langle \Delta^{+} + e^{-} \langle N + \varphi + e^{-}$$

_EW_meeting

- Allows extraction of low energy constant, d_Δ, related to hadronic parity violation

$$A_{PV}^{\square} \langle \frac{d_\Delta M_N}{\Lambda_X}$$

- Two sets of data gives two values of d_Δ
- Q_{weak} values are centered at $d_\Delta = 0$ to show expected precision

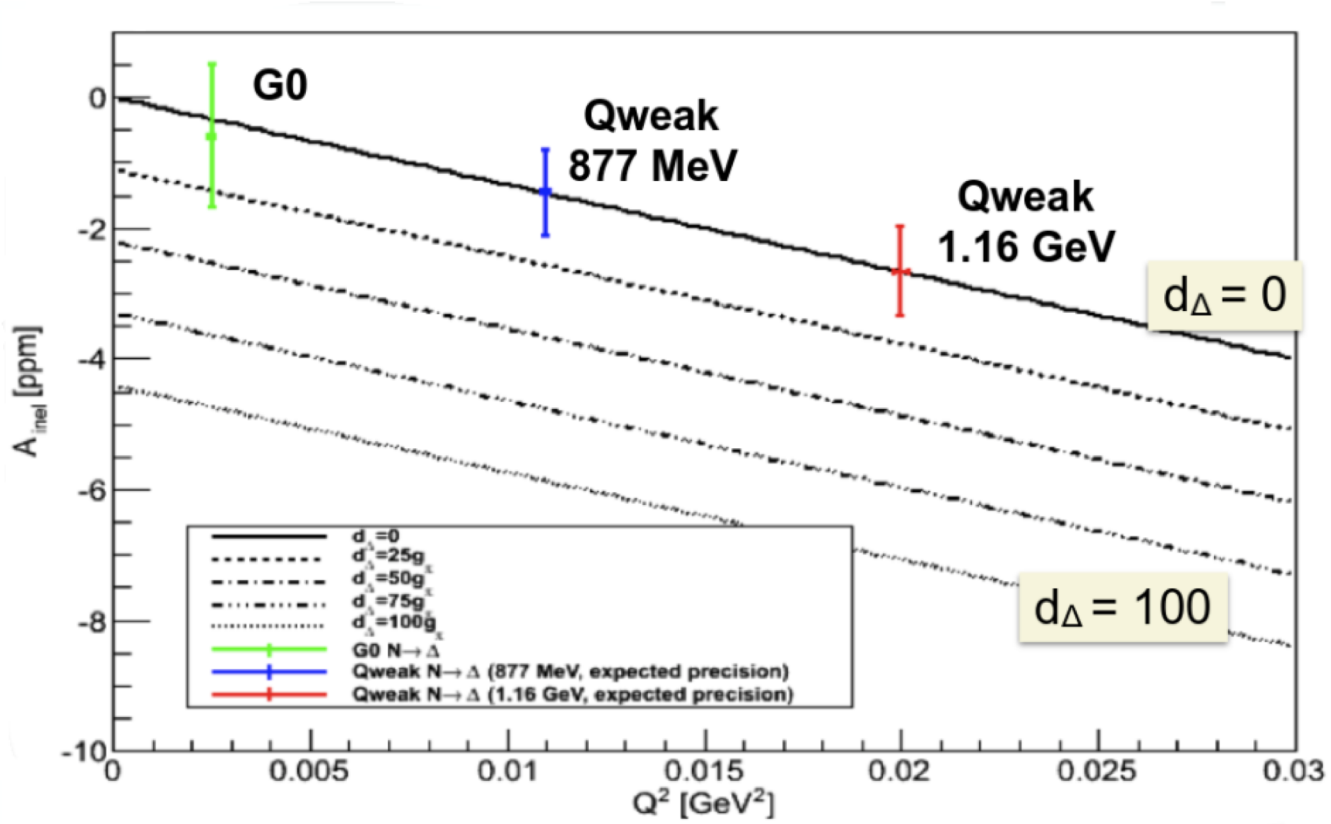

Isovector Axial Form-Factor

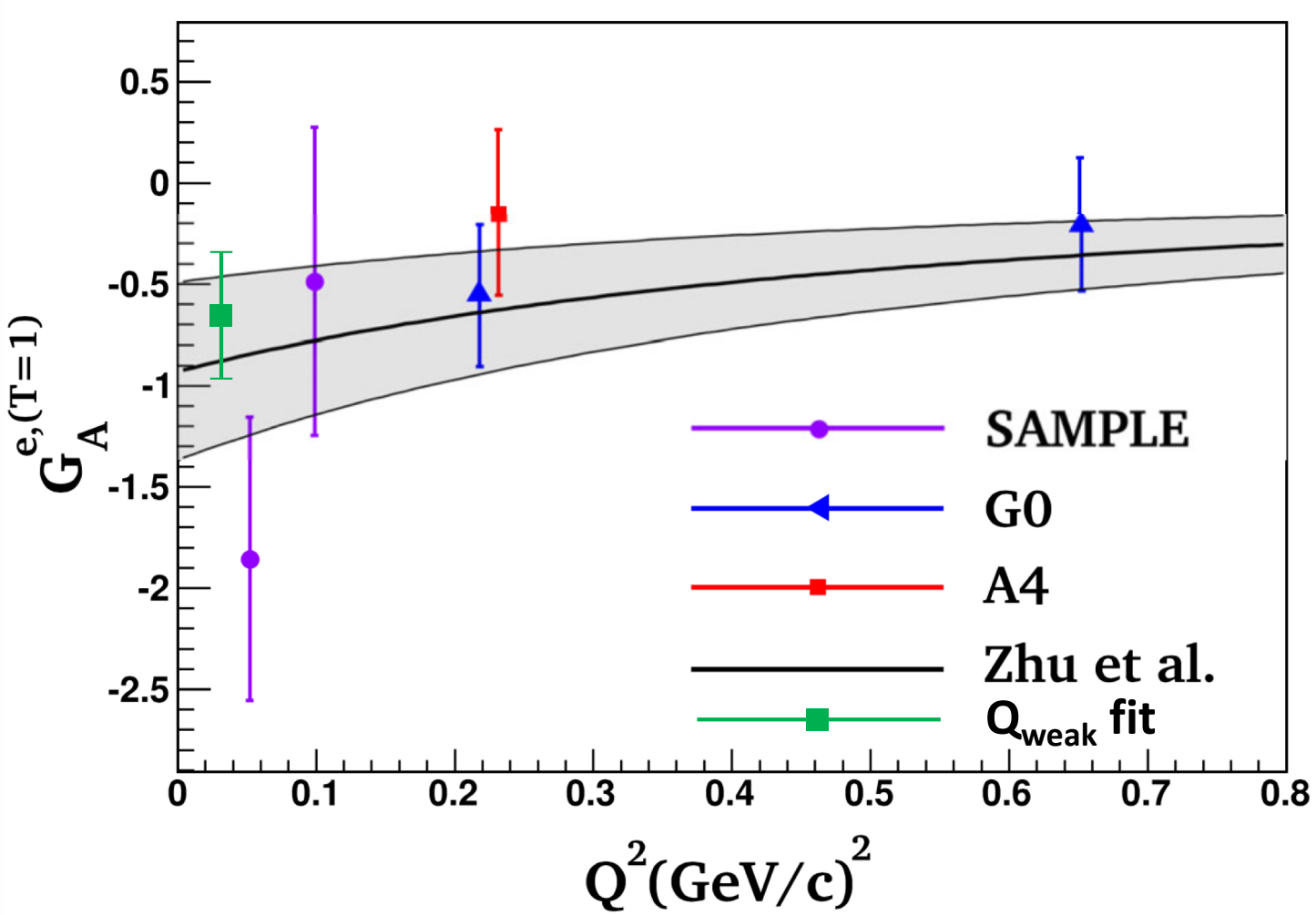

Figure adapted from D. Balaguer Rios *et al.* (PVA4)

Global fit including Q_{weak} is in good agreement with theory

[S.L. Zhu, S.J. Puglia, B.R. Holstein, M.J. Ramsey-Musolf, Phys. Rev. D **62**, 033008 (2000)

]

Secondary Scattering

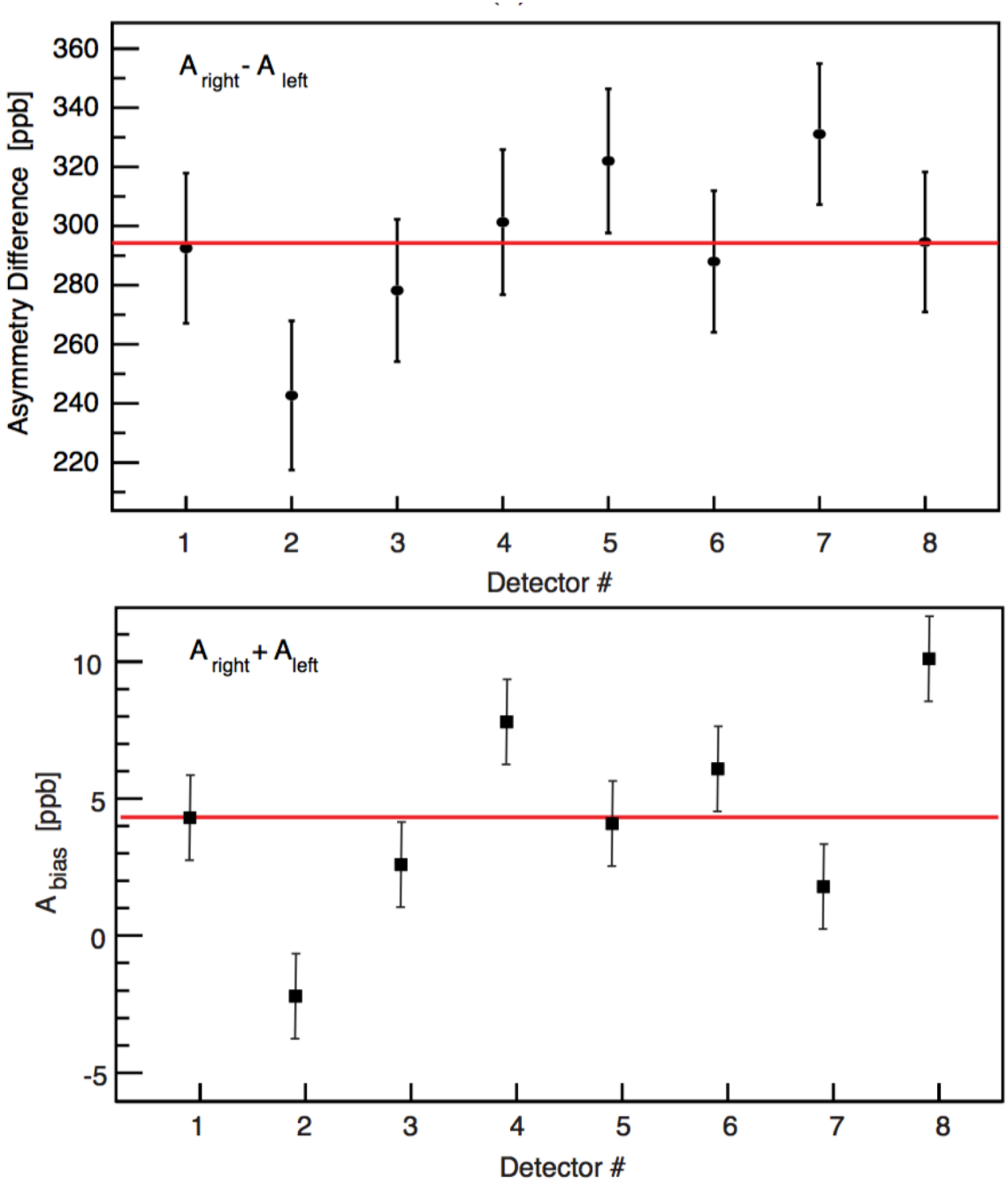

Beamline Background

Concern: Small-angle scattered beam interacting with downsteam beamline components

∴ small-aperture W-Cu "beam collimator'' (1.6 kW deposited power)

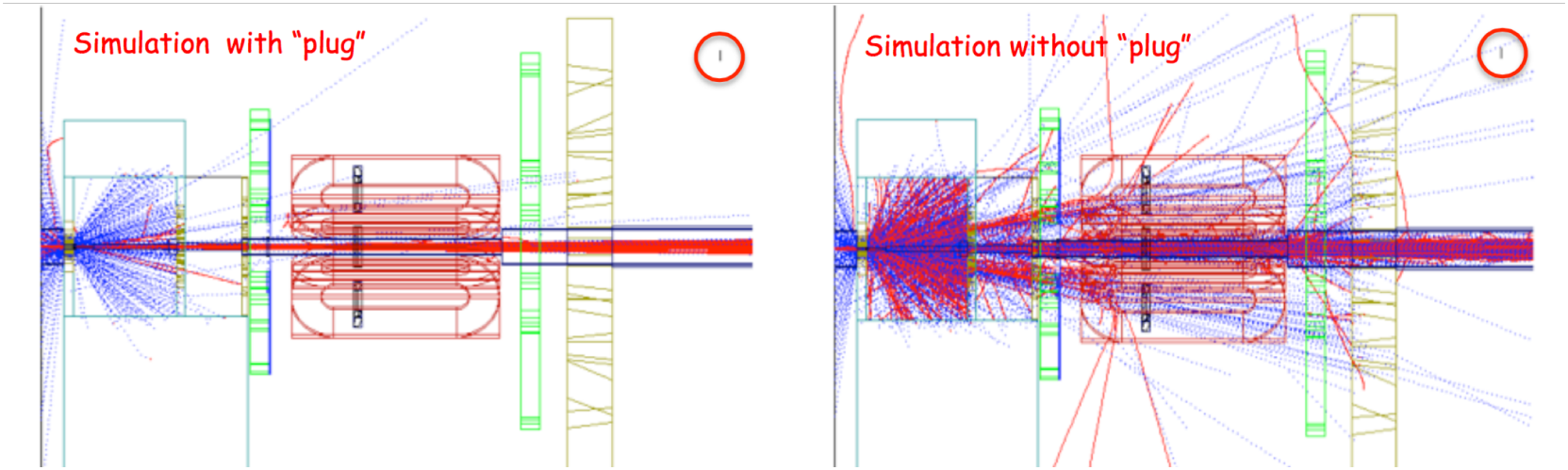

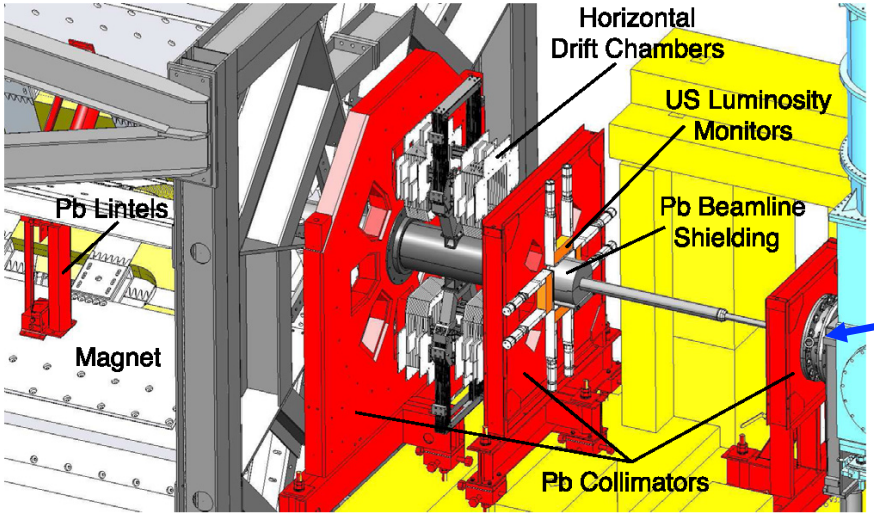

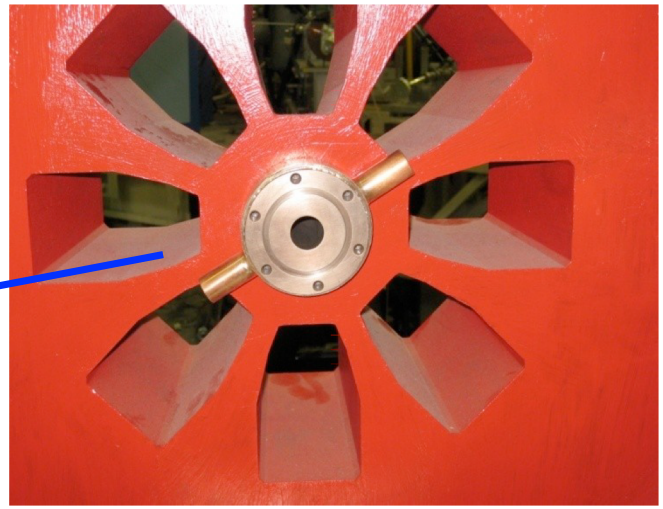

Beamline Background: Halo

Beam Halo:

- measured beam outside of 13 mm diameter (intrinsic beam spot 150 μm)
- typically 10^{-7} to 10^{-6} of beam, but varied up to 10^{-3} in uncontrolled manner.
- could interact in beam collimator, generating backgrounds in Main Detector

Measured directly by blocking signal electrons at primary collimator:
Typical background yield: 0.2% of signal

But: Halo had helicity-correlated component (position and/or intensity)

Large halo asymmetry (up to 20 ppm) scaled down by small fraction (0.2%)

Was largest systematic error in our "Run 0" published result (23 ppb).

Causes helicity-correlated beam sensitivities measured using linear regression to be unstable and to differ from the (stable) sensitivities measured using driven beam motion.

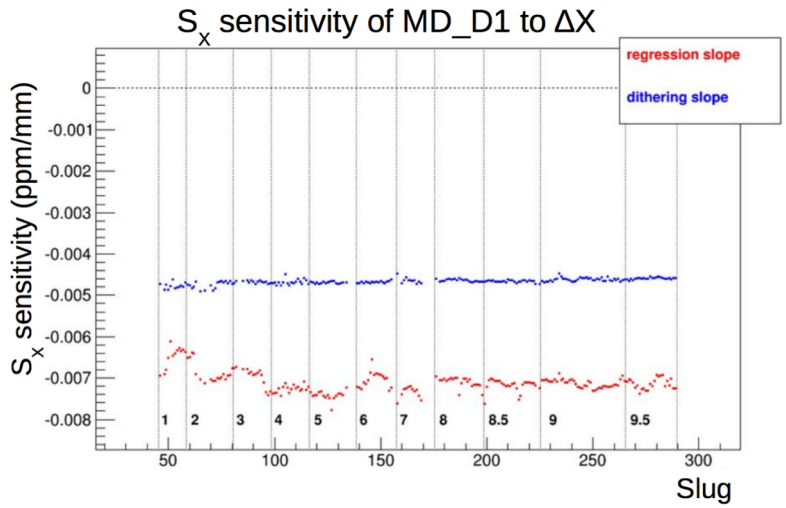

Beamline Background: Monitors

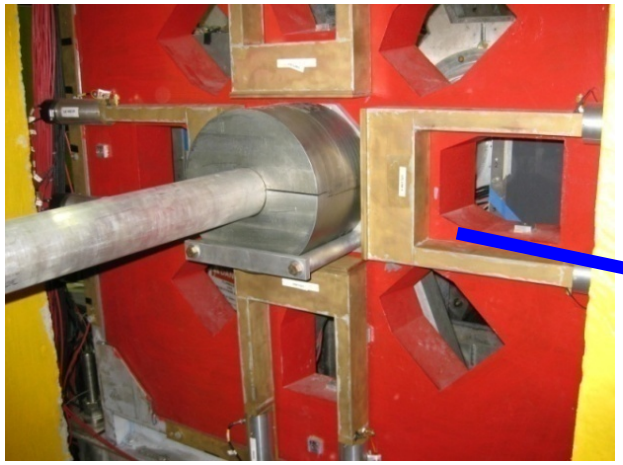

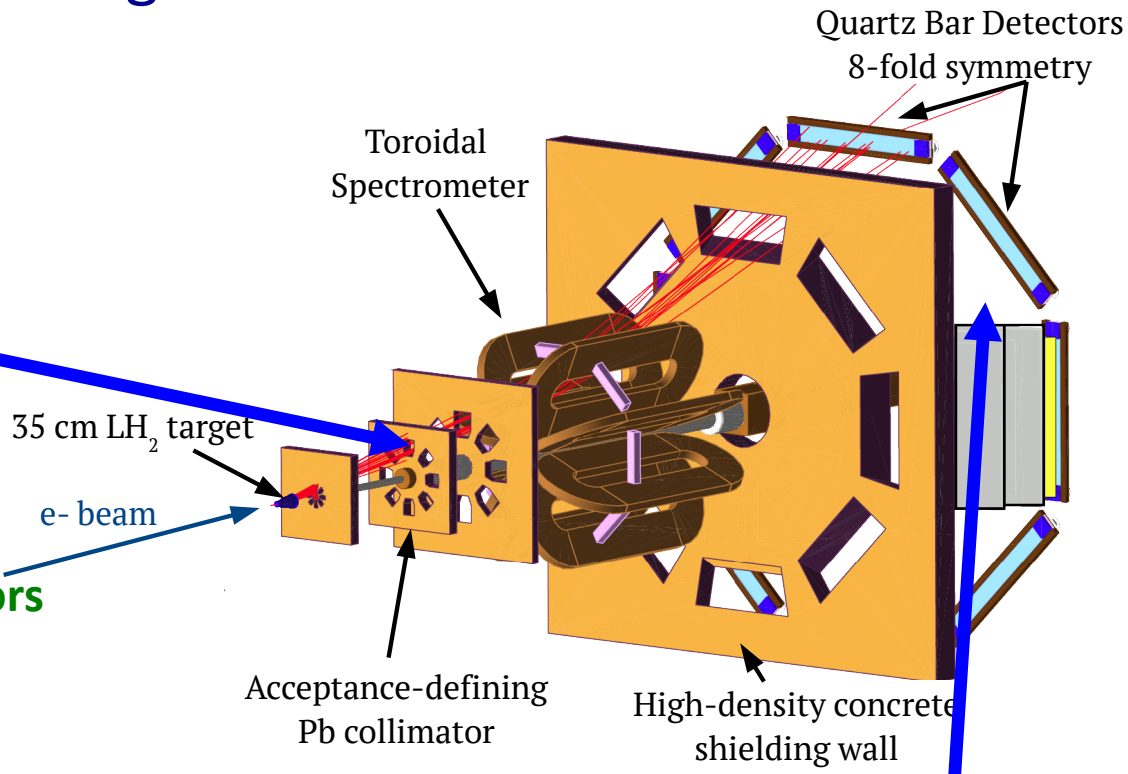

Qweak upstream luminosity monitors

~ 50% of their signal comes from "beamline background"

Qweak diffuse background monitors

- in focal plane at locations where minimal direct signal
- ≈ 10 – 70% of signal from "beamline background"

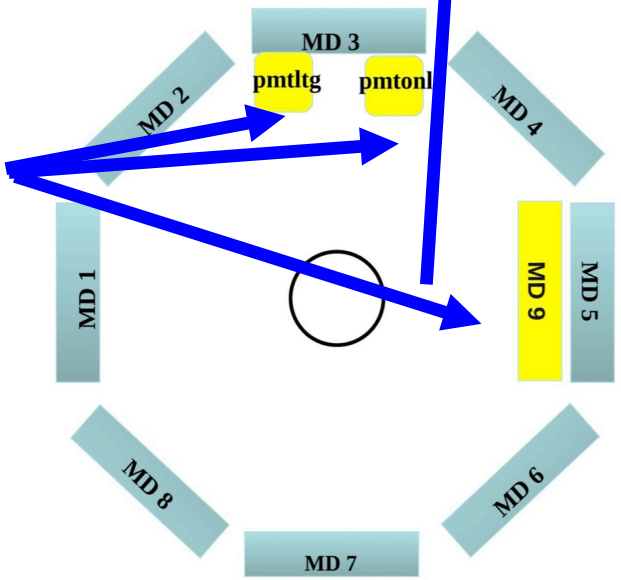

Background detectors measured large (up to 20 ppm) false (only partly cancels with slow reversals) asymmetries

Beamline Background: Correlations

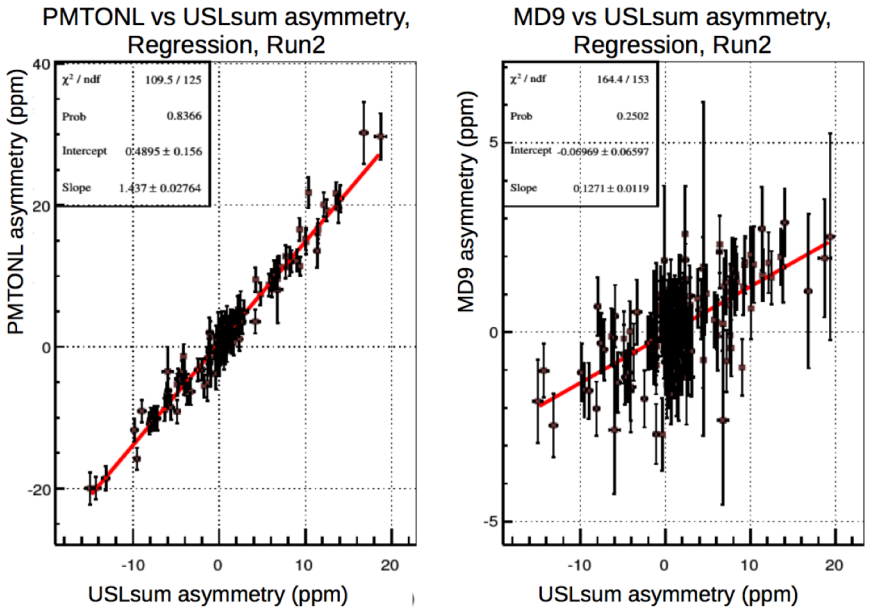

Asymmetries from different background detectors highly correlated

1) Measure Main Detector to Background Detector asymmetry correlation during data-taking (long time-scale averaging)

2) Confirm correlation with blocked-octant study.

3) Using correlation slope and background detector asymmetry, make corrections

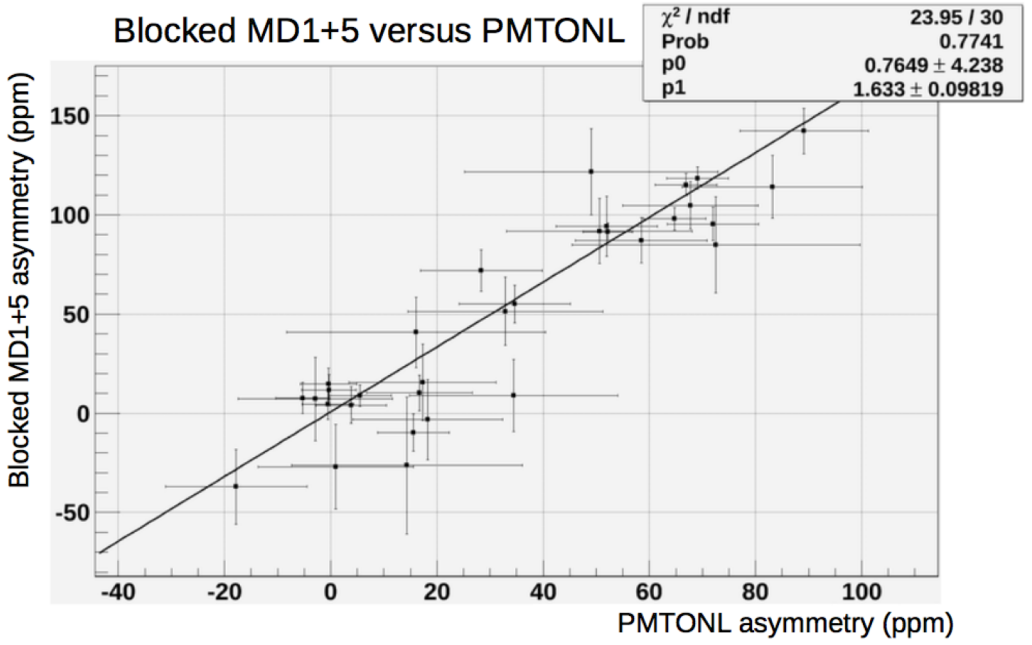

Beamline Background: Corrections

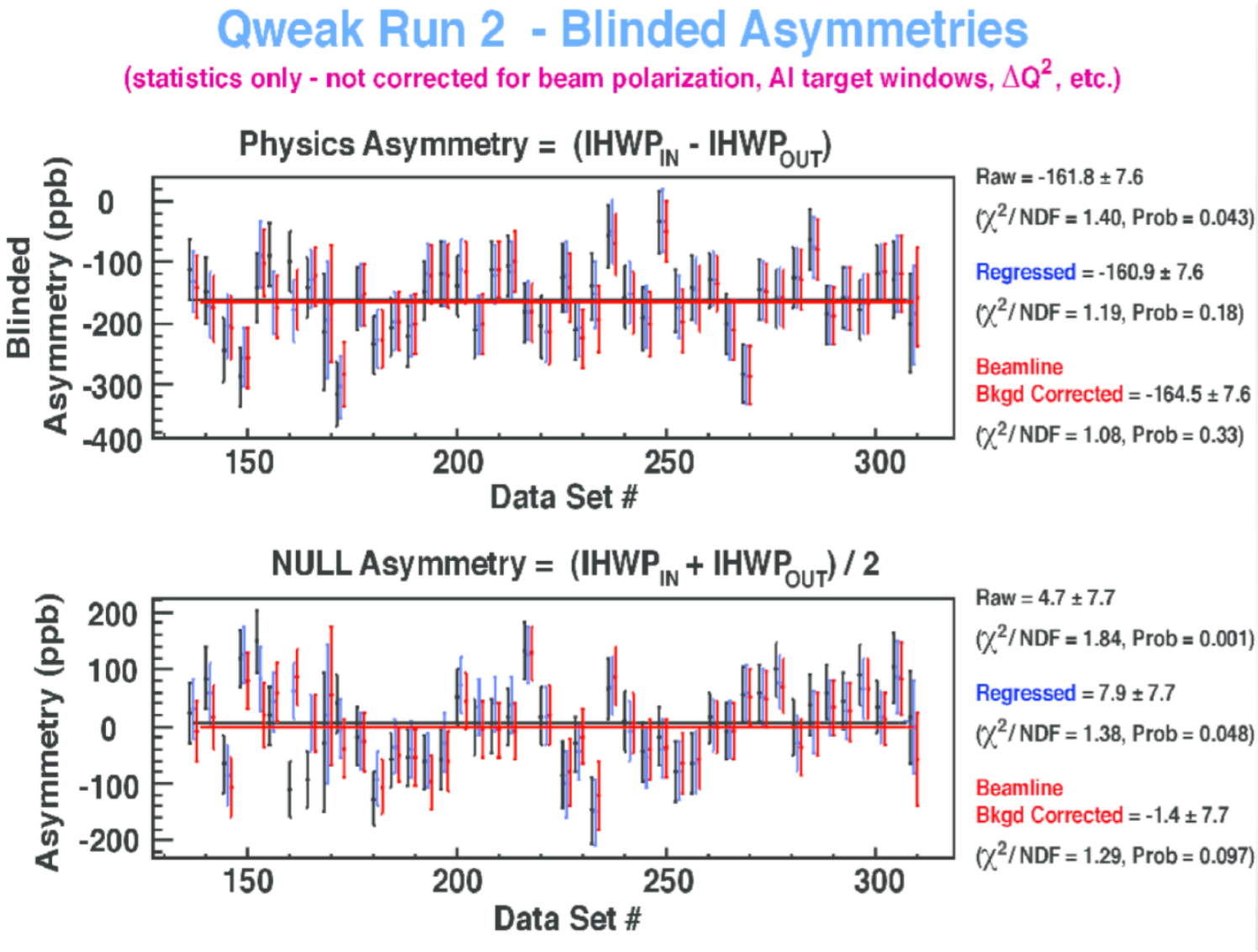

Correcting for beamline background improves statistical consistency of data
(correction size: 3.6 ppb)

Target Windows

Dilution:

- Reduce beam current to $< 1\ \mu$A
- "Counting mode" measurement of rates from empty target and full lH_2 target
- Simulation to account for radiative effects on window signal due to hydrogen

Dilution uncertainty 2.8% (relative). Errors shared equally between:

- BCM calibration
- Detector deadtime (unexpectedly large)
- Simulation

Radiative Corrections to **Asymmetry:**

- Simulation to account for small (8%) kinematic shift in asymmetry for upstream Al window, due to presence of lH_2

Net target window correction: 5% relative error (on 25% correction): 1.2% error, dominated by statistics on Al asymmetry determination

Secondary Scattering: Mott asymmetry

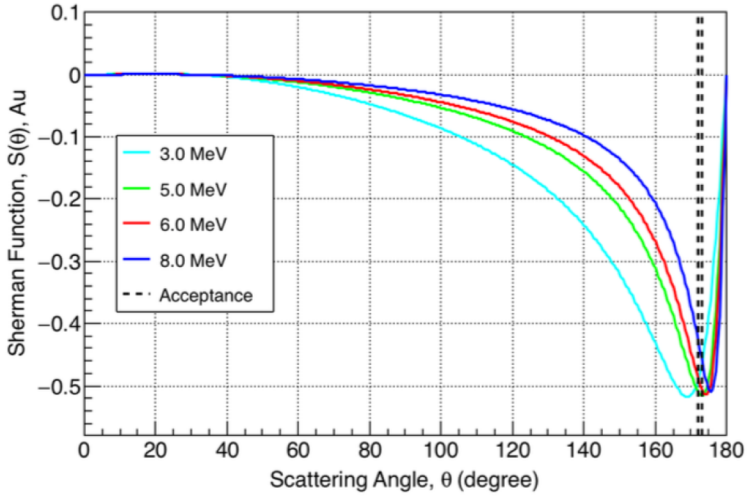

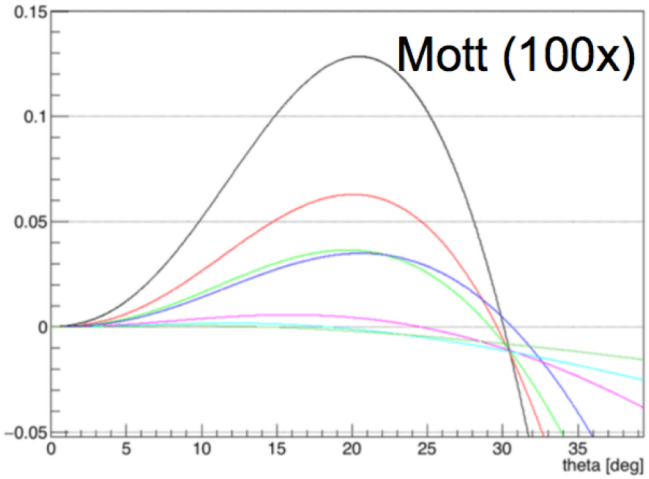

Roca-Maza, Horowitz

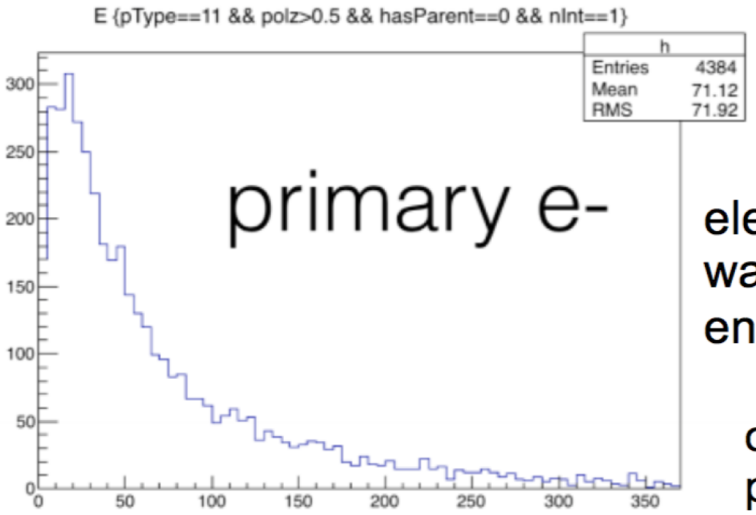

electrons radiate way down in energy….

only ~40% survive
peak E ~20 MeV

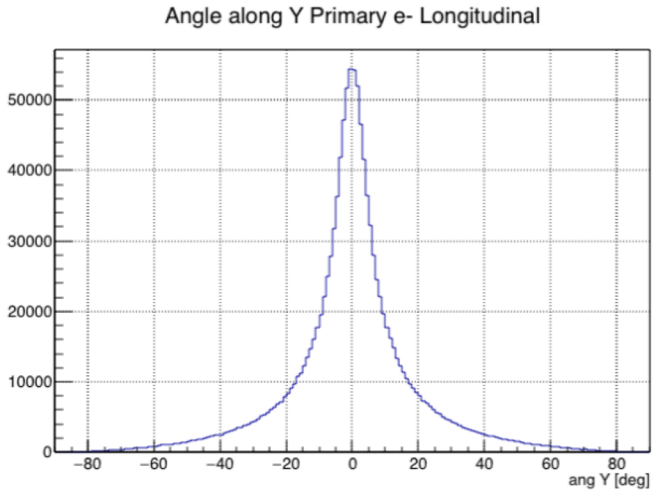

…and scatter a lot

>3MeV:
11% are >30°
6% are >40°

Upstream Luminosity Monitors

Four symmetrically placed quartz blocks (read out with 2 lightguides each) placed on the primary, defining collimator (Collimator #2)

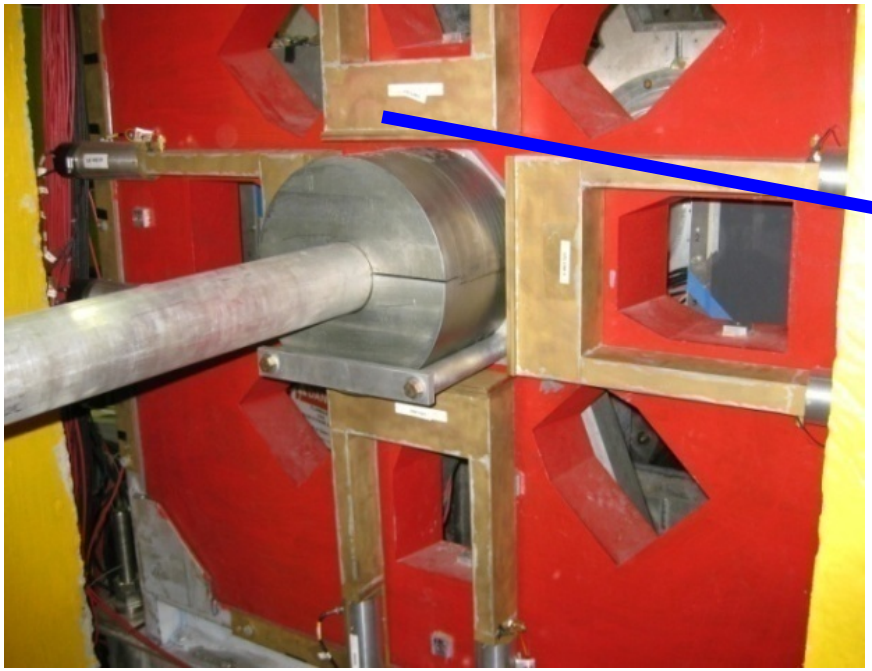

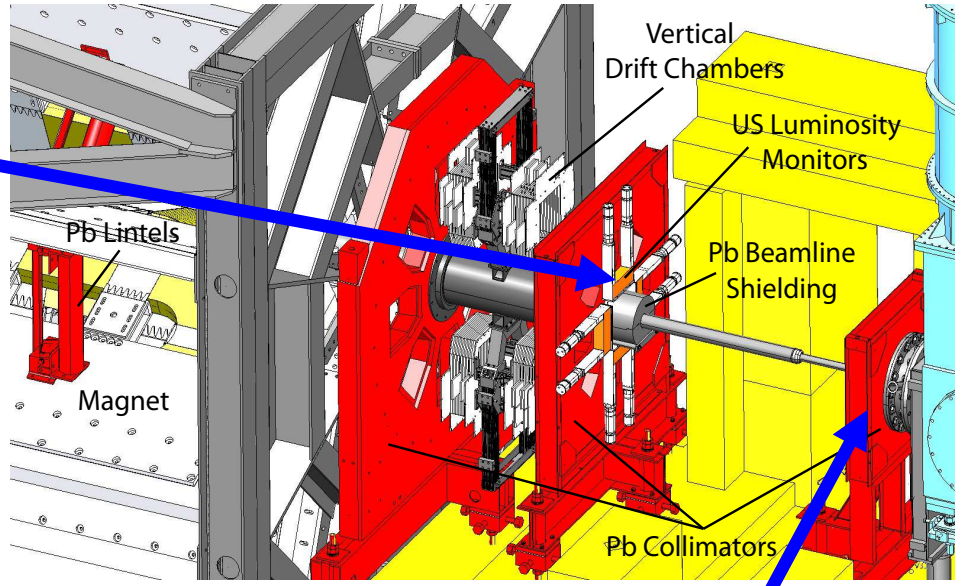

Designed to primarily detect ~ 50 MeV Moller electrons (~ 100 GHZ rate@ 180 μA)
but (from octant blocker studies) ~ 50% of their signal remained when their own octant was blocked – presumably the bulk of this comes from incompletely contained showers in the "tungsten plug"

“Diffuse” Background Detectors

Diffuse background detectors were placed in superelastic regions of the focal plane to monitor soft backgrounds.

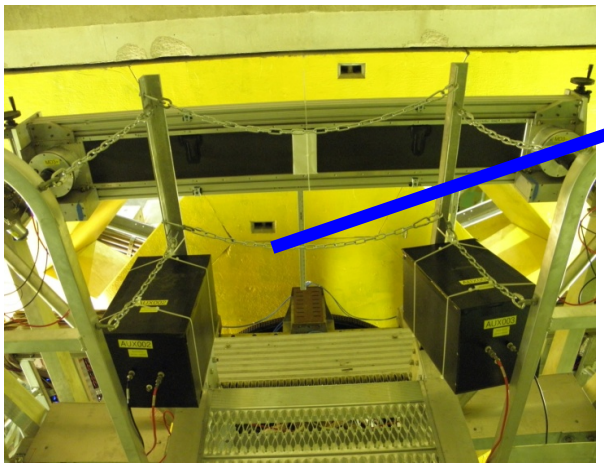

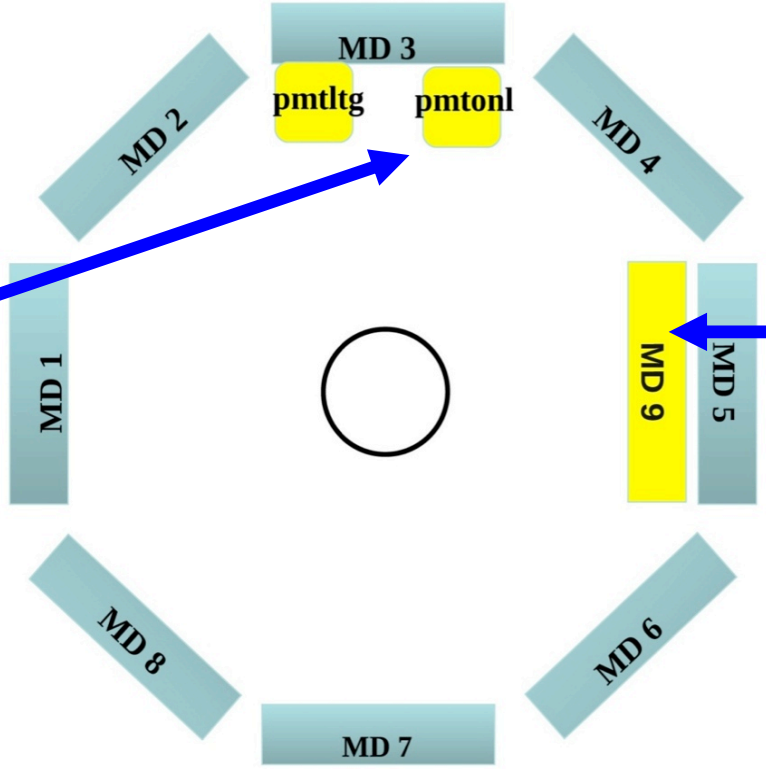

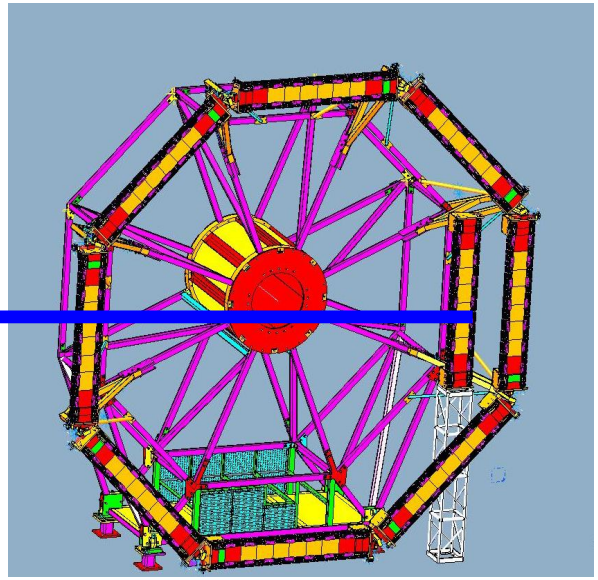

PMTONL: Box with a standard 5 cm Qweak PMT Only

PMTLTG: Box with a standard 5 cm Qweak PMT coupled to only lightguide

MD9: Full Qweak main detector assembly (identical to the other eight)

Helicity-Correlated Halo

Why did the “beam halo” develop helicity-correlated beam properties (charge and position) that were significantly larger than the “core” beam?

Study at end of run in injector region: narrow down chopper slits from their usual wide open setting to explore helicity-correlated charge as a function of longitudinal position in the beam bunch.

After chopper

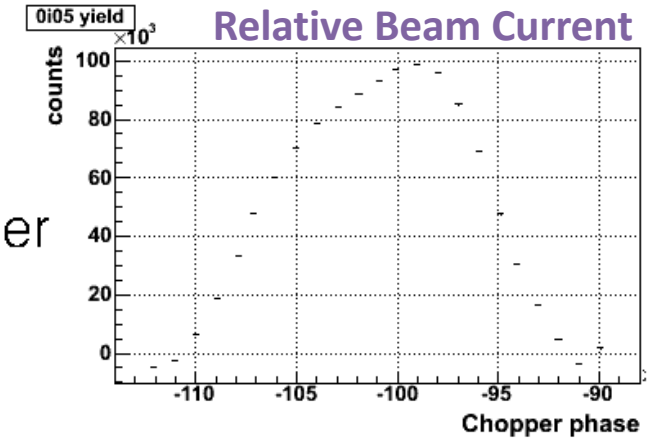

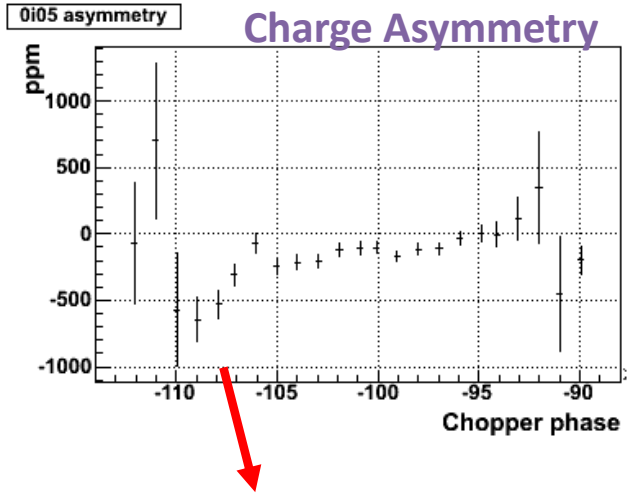

Charge asymmetry is much larger at lagging temporal edge than in core of beam.

Very different helicity-correlated beam properties in the leading/trailing edges of the electron beam bunch can potentially translate into large helicity-correlated beam properties in the beam halo observed in the experimental hall.

PVDIS (eD) 6 GeV JLab

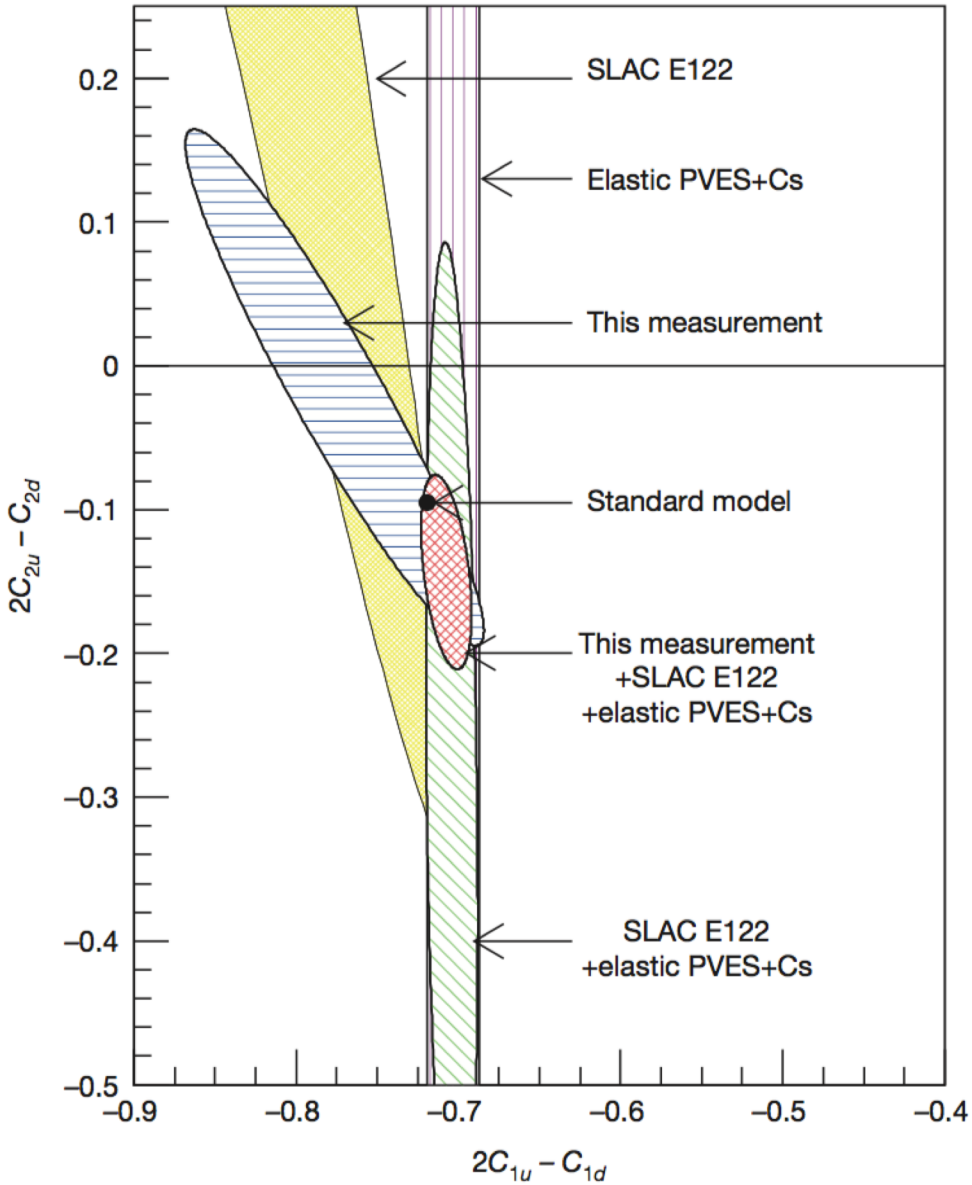

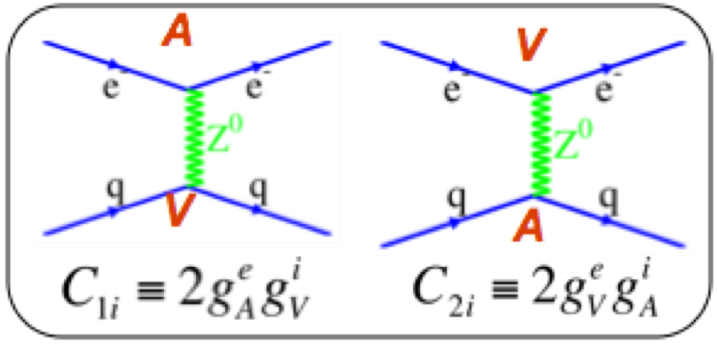

Small θ Large θ

$$C_{2u} = -\frac{1}{2} + 2\sin^2\theta_W \quad C_{2d} = \frac{1}{2} + 2\sin^2\theta_W$$

$$A_{\rm exp} = -160 \pm 6.4({\rm stat}) \pm 3.1({\rm sys})\ {\rm ppm}$$

$$A_{\rm SM} = -158.9 \pm 1.0\ {\rm ppm}$$

Spokespersons:
Xiaochao Zheng (U. Virginia),
Paul E. Reimer (ANL)
Bob Michaels (JLab)

Nature 506, (2014) 67

Moller-Compton-Moller

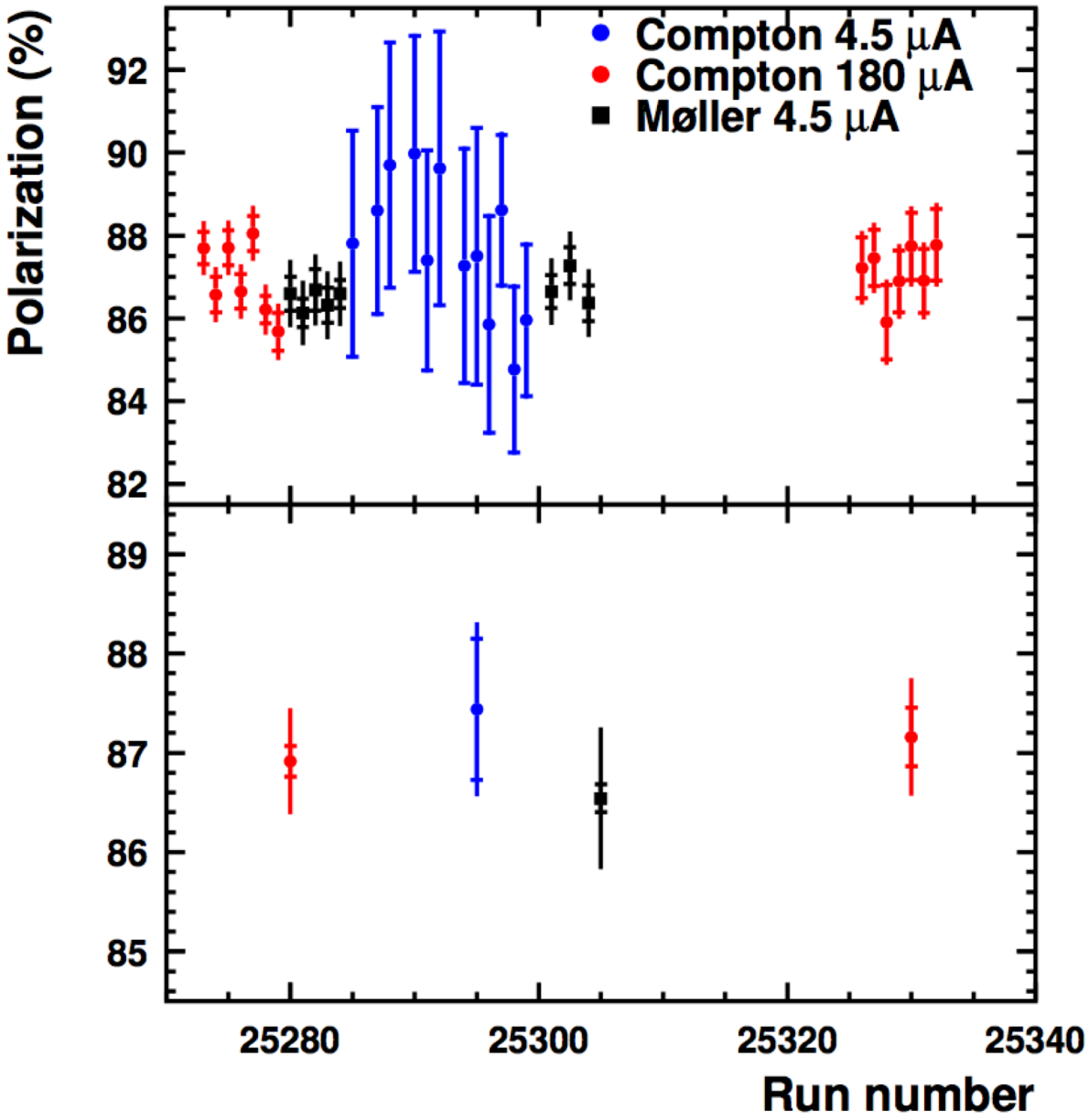

Polarization is independent of beam current

The Qweak Apparatus